UNITED NATIONS UNIVERSITY
UNU-GTP
Geothermal Training Programme

Orkustofnun, Grensasvegur 9,
IS-108 Reykjavik, Iceland

Reports 2016
Number 30

OPTIMISED PIPELINE ROUTE DESIGN FOR CONNECTION OF A MAKE-UP PRODUCTION WELL: CASE STUDY OF WELL OW-906 FOR OLKARIA IV POWER PLANT, KENYA

Daniel Wanga Odongo
Kenya Electricity Generating Company Ltd. - KenGen
P.O. Box 785-20117, Naivasha
KENYA
dwanga@kengen.co.ke

ABSTRACT

Over the course of the life of a geothermal project, the steam flow will generally decline due to natural drawdown effects or changes in the reservoir as the resource is exploited. This requires that from time to time, the steam is made up by connecting additional wells to the existing steam gathering system. This process can be very challenging given the constraints offered by an already existing framework. Moreover, it requires that proper selection of the pipeline routing and tie-in points is done to ensure that the make-up well is connected in the most cost effective manner. Consideration must be given to the existing separator stations and pipelines, to ensure that there is no additional expensive construction of steam field infrastructure, unless utterly necessary. Focus should be placed on ensuring that existing spare capacities are first exhausted before more infrastructure is put up. This work attempts to give a preliminary outline for the impending connection of well OW-906 to the already existing Olkaria Domes steam field that serves the Olkaria IV plant in Olkaria, Kenya. The main focus area is the use of Variable Topography Distance Transform (VTDT) method to identify the optimal pipeline routes that would allow connection of make-up wells as cost effectively as possible. This work shows that the use of VTDT has guided the selection of the optimal route for connection of make-up well OW-906. The cheaper option is construction of a new separator station at an optimal position near the well head and then connecting the steam pipeline to the nearest main steam pipeline from separators SD1 and SD4. Brine reinjection is also to be channelled to the nearest reinjection well OW-906A. This work is intended to provide a guide for the future when new wells make-up wells are to be connected to an existing steam gathering infrastructure.

1. INTRODUCTION

1.1 General

The Olkaria geothermal resource is located in the Kenya Rift valley, about 120 km from Nairobi, the capital city of Kenya. Geothermal activity is widespread in the Kenyan rift and 14 major geothermal prospects have been identified (Figure 1). The Olkaria geothermal field is inside a major volcanic

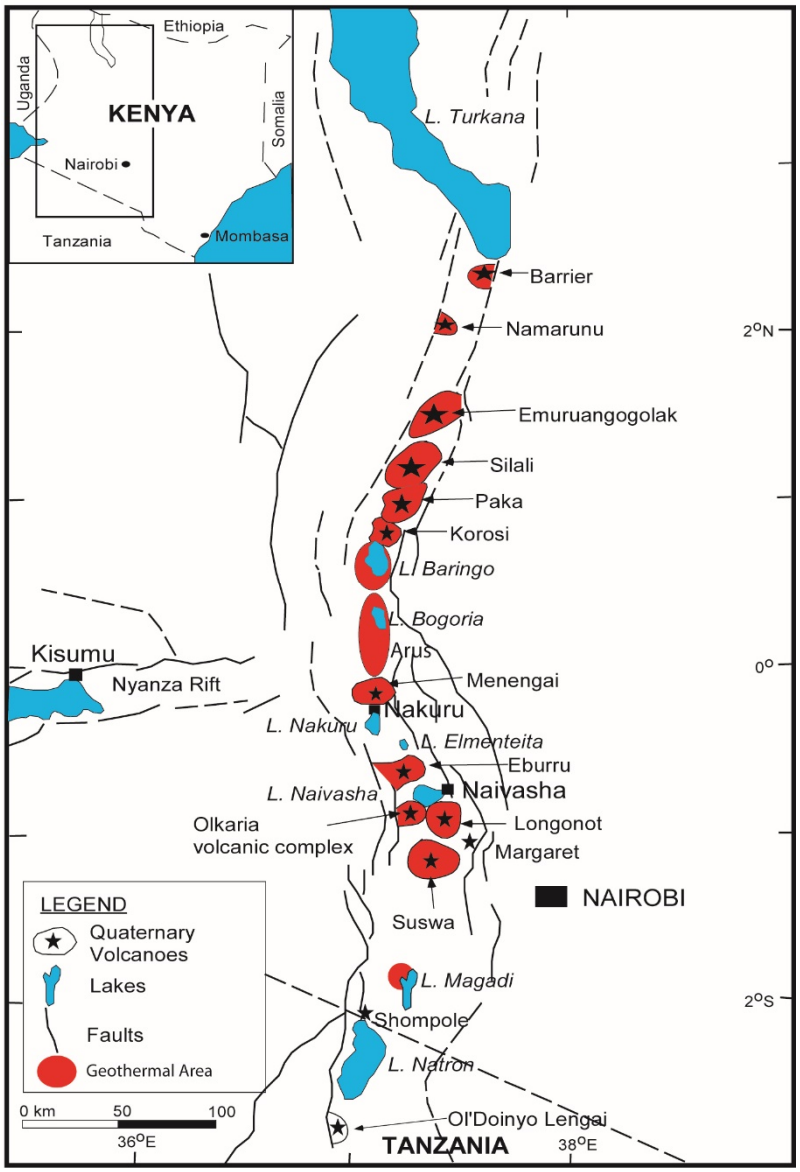

FIGURE 1: Greater Olkaria geothermal area within the Great Rift Valley of Kenya (Ofwona, 2010)

complex that has been cut by N-S trending normal rifting faults. It is characterized by numerous volcanic rhyolitic domes, some of which form a ring structure, which has been interpreted as indicating the presence of a buried volcanic caldera (Mannvit, 2012). Olkaria is surrounded by further geothermal prospects, such as Suswa, Longonot and Eburru (Figure 1).

Exploration of the Olkaria geothermal resource started in 1956 with deep drilling commencing in 1973. A feasibility study in 1976 indicated that development of the geothermal resource was feasible and consequently a 30 MWe power plant was constructed (Ouma, 2010). Three power plants were installed in the field before 2014, producing electricity; Olkaria I with 45 MWe capacity, Olkaria II with 105 MWe capacity and Olkaria III with 120 MWe capacity. The first two are operated by KenGen, the largest power producer in Kenya owned 70% by the government and 30% in private hands. The third plant is operated by OrPower 4, an independent power producer (IPP). The Olkaria I power plant consists of 3 units commissioned between 1981 and 1985 while Olkaria II, which also has 3 units, was commissioned between 2003 and 2010. The Olkaria III power plant was commissioned in two phases between 2000 and 2012. In addition, the geothermal resources of the northwest part of the Olkaria area are utilized both for direct heat and small scale electricity generation by the Oserian flower farm. KenGen has also recently started operating wellhead units of 2-5 MWe capacity which are now (mid 2016) generating about 70 MWe from 14 wells. Olkaria IAU and Olkaria IV are the latest power plants to be commissioned within the Olkaria geothermal field. Olkaria IV plant was commissioned in June 2014 as part of the Greater Olkaria 280 MW project that represented the largest one-off geothermal development project in the world. It is a 140 MWe plant utilising 2×70 MWe turbines. Olkaria IAU is an extension of Olkaria I, commissioned in December 2014, and also with 140 MWe utilized through 2×70 MWe turbines (units 4 and 5). The parts of the Olkaria geothermal field being utilized or under development have been subdivided into sectors that include Olkaria East (Olkaria I), Olkaria Northeast (Olkaria II), Olkaria West (Olkaria III) and Olkaria Domes (Olkaria IV).

The Olkaria IV plant is a single-flash plant utilising 2×70 MWe condensing double-flow double entry turbines, direct contact condenser and a wet cooling tower. Design turbine inlet pressure is 6 bar and

condenser pressure 0.075 bar. The steam field consists of 21 production wells, 7 brine reinjection wells and 2 condensate reinjection wells.

The steam field was initially designed to be operated at 7 bar. An optimisation study carried out later by Mannvit Consortium (Mannvit, 2012) recommended that the steam field pressure be raised to at least 11 bar to limit the effects of silica scaling. This was due to the fact that the wells serving these power plants were drilled to a depth of 3000 m on average. This was much deeper than the earlier average well depths of 1200 m and 2200 m for developed fields of Olkaria East and Olkaria Northeast, respectively. They therefore tapped from a more silica-rich environment due to the higher reservoir temperatures at depth. This fact had not been fully considered during the design phase. A separation pressure of 6-7 bar would cause silica supersaturation during flashing and therefore encourage silica scaling that would ultimately clog the sub-surface piping. This separation pressure change effectively reduced the available steam by reducing the steam reserve margin. KenGen has already implemented this by introducing control valves between the steam field and the power plant to maintain the steam field pressure at 12 bar. The result of this was as indicated in Table 1.

TABLE 1: Olkaria IV steam flow effects due to separation pressure change

	Separation pressure 6-7 bara	**Separation pressure 12 bara**
Total available steam flow (kg/s)	322	308
Plant steam demand (kg/s)	280	280
Reserve steam margin (kg/s)	42	28
Reserve steam margin (%)	15	10

The reduction in the reserve steam margin limits the flexibility of carrying out any maintenance work or dealing with emergencies. In addition, five of the production wells serving the Olkaria IV plant are wells that are not self-starting and would need to be stimulated if there is a shutdown.

The brine reinjection capacity of the wells in Olkaria IV steam field was also highly understated. Seven reinjection wells were allocated for brine reinjection but after commissioning of the system, it was confirmed that the 236 kg/s of brine generated from the separation stations of the field could comfortably be taken care of by 3 wells. Figure 2 shows the location of well OW-906 in the Olkaria IV steam field.

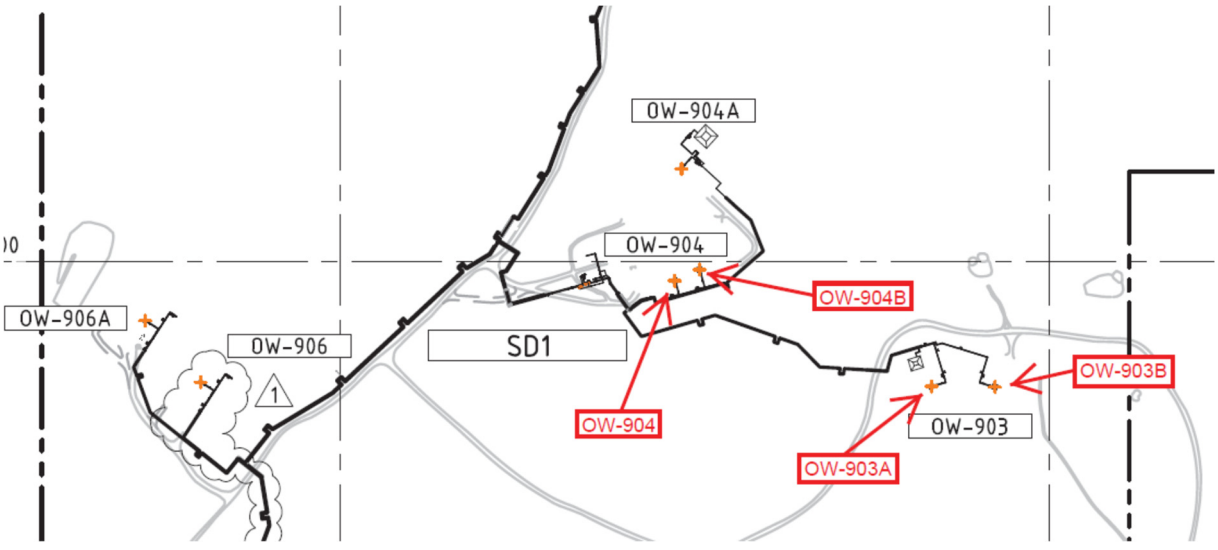

FIGURE 2: Location of well OW-906 within Olkaria IV

OW-906 was initially intended to be a production well but was connected as a reinjection well due to understated reinjection capacity. This work intends to redesign this well as a production well using the pipe design optimisation tools to find the most cost effective pipe route, pipe diameter, separator positioning, reinjection well to use and reinjection pipeline route.

1.2 Objectives

The overall goal of this work is to develop a methodology that can in the future be used to connect make-up wells optimally, considering that make-up wells would be connected within already existing infrastructure which would offer several obstacles to the intended pipeline routes. This would require that the route and placement of facilities is optimised to limit cost of connection of these wells. The main objectives of this project are the following:

- Obtain the optimal pipe route for two-phase, steam and brine to connect well OW-906 to the existing Olkaria IV steam field;
- Obtain optimal separator location for the well;
- Obtain optimal reinjection pipeline route and well for its brine;
- Determine optimal pipe sizes for two-phase pipeline and steam;
- Predict the expected pressure drops for two-phase, steam and brine pipelines;
- Ultimately increase reserve steam margin of Olkaria IV power plant.

1.3 Literature review

Geothermal wells generally produce a mixture of steam and water. The mixture is then separated into distinct phases of steam and water with minimum pressure drop. The steam is then conveyed to the power plant and the brine to suitably located reinjection wells by gravity or by pumping. A typical 30 MW plant would require about 5-6 production wells and 2-3 reinjection wells (DiPippo, 2016). These wells may be drilled on sites distributed across the field or several may be drilled from a single well pad using directional drilling. In either case, a piping system is needed to gather the fluids and transport them to the powerhouse for steam and to the points of disposal for water. The steam gathering system can therefore be defined as a network of pipelines from production wells to separator stations, separator stations to power plants for steam, separator stations to reinjection wells for separated brine, separator vessels and accompanying equipment to allow for safe operations (Onyango, 2015).

Two-phase flow
Two-phase flow in horizontal pipelines can be in different regimes. (Zarrouk and Purnanto, 2016). Bubble flow is formed when there are steam or gas bubbles moving at approximately the same velocity as the liquid. Plug flow is formed when there are alternating plugs of liquid on the upper part of the pipe. Stratified flow is formed when liquid flows on the lower part of the pipe with the steam or gas phase flowing on the upper part of the pipe. Wave flow is similar to stratified flow but the steam or gas phase moves at a higher velocity causing disturbances on the interface causing waves. Slug flow is formed when the wave of the liquid is picked up by the faster moving steam or gas and then moves faster than the average liquid velocity. Annular flow is formed when steam or gas moves at a higher velocity in the centre of the pipe, surrounded by a slower moving liquid on the walls of the pipe. Mist flow is formed when almost all the liquid is entrained as droplets in the steam or gas. Figure 3 shows two-phase flow patterns in horizontal flow.

Flow characteristics vary from annular to open channel depending on the ratio between the steam and the water. Slug flow generates a huge dynamic load and should be avoided. Baker and Mandhane maps can be used together with superficial velocity to predict the flow pattern in a two-phase pipe. Pressure drop in two-phase flow is very difficult to determine. However, correlations have been used with a fair amount of accuracy. Common methods that have been used are homogeneous method, Harrison-

Freeston method, Zhao-Freeston method, Lockhart-Martinelli method, Friedel method and Brill-Murkerjee method.

Steam flow

Pipelines are generally larger due to the higher specific volume of steam. Steam velocity is typically 30-40 m/s and pressure drop can accurately be determined using the Darcy-Weisbach equation and Colebrook friction factor equations. Pipelines are also having drain pots installed to remove condensate that develops in the steam pipelines as a result of pressure drops and losses as the steam flows along. This also helps to keep the steam as dry as possible, typically between 99.5% and 99.9% dry (Zarrouk and Purnanto, 2014).

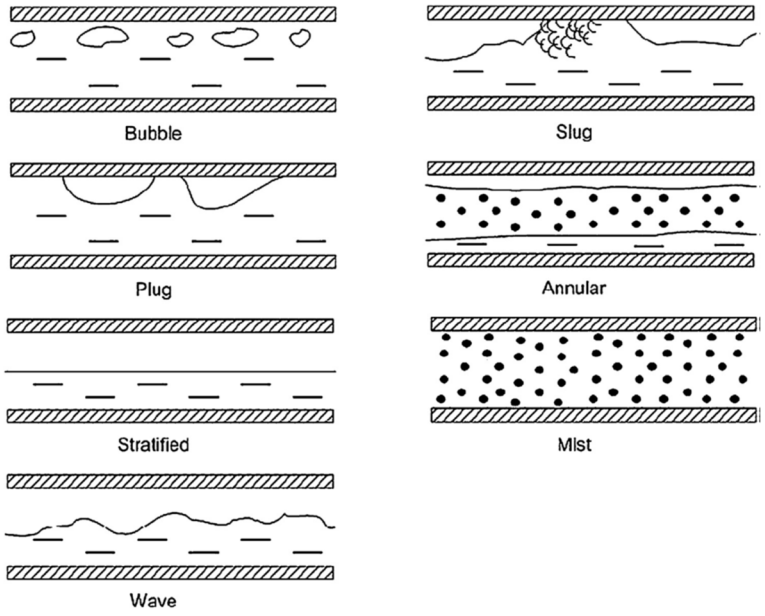

FIGURE 3: Two-phase flow patterns in horizontal flow (Zarrouk and Purnanto, 2014)

Brine flow

Brine leaving the separator is usually in saturation and care must be taken to ensure that no point along the brine pipeline is below the saturation pressure. Reinjection wells are therefore designed to gain static head (Henriquez and Aguirre, 2011). Due to the low elevation, brine reinjection wells experience the highest hydrostatic pressure. Brine flow can be anything between open channel flow and full flow depending on the geometry of the pipe. The slope required for open channel flow can be determined using the Chezy's or Manning equation. Full flow velocity is usually on the order of 2-3 m/s and the pressure drop can be estimated using the Darcy-Weisbach equation and Colebrook friction factor equations. In addition, brine pipe design should also consider erosion, corrosion, silica scaling, brine residence time, dynamic load from potential slug flow situations and provision for draining the load whenever it is required.

Pipe routes and separators

Geothermal pipe route selection has been studied extensively with algorithms developed to optimise pipe routes. One of them is the Variable Topography Distance Transform (VTDT) by De Smith (2005). Kristinsson (2005) used the VTDT to determine shortest possible route for geothermal pipelines. More work was done by Kjaernested (2011) that included incorporation of visual effect optimised codes to the VTDT algorithms. This was applied in a geothermal field in Iceland with good results. Multiple Weight Distance Transform (MWTD) was initially suggested by Kristinsson (2005) to optimally locate separators and power plants. This algorithm was later used by Kjaernested (2011) to locate separators in the Hverahlíd geothermal field.

Geothermal separators are classified as either horizontal or vertical (DiPippo, 2016). The vertical cyclone design is based on reports and experience in Wairakei and Kawerau in the 1950s and 1960s by the modelling work of Lazalde-Crabtree (1984). Horizontal separators are flash vessels where the mixture will enter from the top and travel horizontally while flashing occurs. The main concern is to have the mixture velocity sufficiently lowered to give the water particles enough time to settle to the bottom before steam leaves from the top. Separators locations within the production field can be in three ways. Separators can be located near the wellhead taking two-phase fluid from individual wells, they can be at satellite locations collecting two phase fluid from a number of wells or they can be centralised and located close to the power plant and collecting two-phase fluid from long pipelines from all the wells (DiPippo, 2016). Steam and brine pipelines then move from these stations to the power plant and

reinjection wells respectively. The option that is selected depends on various design considerations like pressure drop, cost limits, environmental considerations and pipeline obstacles among others.

The cost of geothermal steam gathering systems depends on a number of factors, the key factor being distances from wells to power plant, flowing pressure of the wells and fluid chemistry. Onyango (2015) puts the estimate of steam gathering systems at about 10% of the overall project cost. Henriquez and Aguirre (2011) estimate the costs to be a lot higher at US$600 to US$1200 per metre, and summarise the cost to be made up of material 30%, fittings 10%, installation labour 25%, installation equipment 10%, pipe supports 15% and management 10%. Hance (2005) estimates the cost at 15-25 USD/inch of diameter, per foot of length for carbon steel which are the most commonly used material. Kalinci et al. (2007) provides estimates of pipe and bends cost and installation cost that indicates that all these costs will generally increase as the nominal pipe diameter increases. Table 2 shows a summary of pipe and pipe bends costs and installation costs for pipe and bends depending on pipe nominal diameter.

TABLE 2: Pipe and bend cost and installation costs (Kalinci et al., 2007)

Pipe nominal diameter (m)	Pipe cost (USD/m)	Pipe installation cost (USD/m)	Pipe bend cost (USD/unit)	Pipe bend installation cost (USD/unit)
0.20	50	30	150	25
0.25	70	45	300	50
0.30	90	55	450	100
0.35	115	79	700	225
0.40	150	110	950	275
0.45	175	130	1350	375
0.50	215	150	1750	403

2. DESIGN CONSIDERATIONS

Successful delivery of geothermal piping design requires a number of structured processes which are customized to the developer and to specific project requirements (Umanzor et al., 2015). These processes may vary but steps shown on Figure 4 appear to be commonly used.

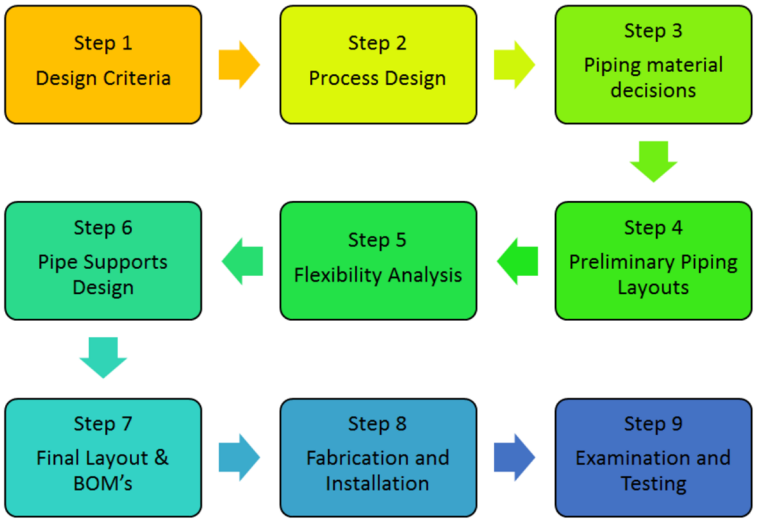

FIGURE 4: Piping design processes (Umanzor et al., 2015)

Step 1: Design criteria.
The client and the designer agree on the design criteria to be applied in the entire project. Relevant criteria such as pipe sizing, layout considerations, insulation methodology, design codes and standards are typical components of this step.

Step 2: Process design
The process design should be advanced at this stage since all the required steam field data and well test reports will have been obtained. This step involves the preparation of heat balance and mass balance equations.

Step 3: Pipe material decision
From the well discharge reports, chemistry of the fluid at the intended operating conditions will determine the materials to be used in this design.

Step 4: Preliminary piping layout
This step is critical to ensure the constructability of the pipeline and that stakeholders are considered to avoid a redoing of the design. Variable topography distance transforms (VTDT) can be used in this stage to get a preliminary route for the pipeline and help to estimate the length of the pipeline.

Step 5: Flexibility analysis
This step uses design software to carry out stress analysis and compatibility of the design to design code requirements. This will normally be done using stress analysis computer packages and models.

Step 6: Pipe supports design
Normally the pipeline will be designed before the supports but the construction is usually the reverse. This requires that the civil engineers are involved early in the process. The loads on the pipe due to thermal and seismic loading can sometimes be unrealistically large due to insufficient flexibility or inappropriate piping layouts and restraints. This must be looked at early to avoid expensive and structurally impractical situations.

Step 7: Final layouts and Bill of Materials (BOM)
After final layouts are agreed from step 4, these can be prepared and the bill of materials also generated from this.

Step 8: Fabrication and installation
The pipe is fabricated and equipment installed. Changes can be made over the course of fabrication but should be only minor.

Step 9: Examination and testing
Pipeline is commissioned and tested. Amongst others, procedures and tests may involve steam blowing and hydro testing.

2.1 Pipe route selection

Pipe route selection depends on the fluid to be transmitted through the pipes (Onyango, 2015). Distance Transforms (DT) is one of the methods that can be used to obtain optimal paths across the landscape. DT is an image processing algorithm which works with a digital binary image that consists of object points and non-object points. The shortest (unobstructed) path across a uniform horizontal or tilted plane is a Euclidean straight line. If the surface is tilted, the surface will have a non-zero path gradient with respect to the underlying horizontal plane (Figure 5 path P_1). Calculating exact Euclidean

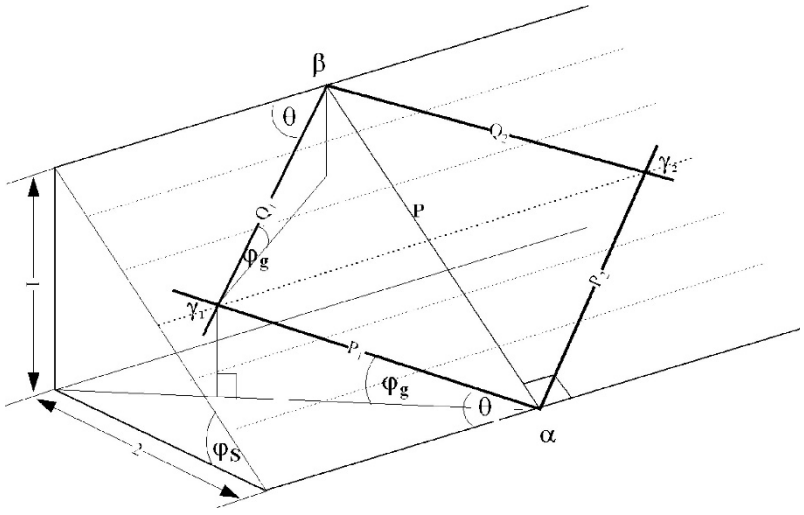

FIGURE 5: Gradient constrained path on a sloping planar surface (De Smith, 2005)

distances can be extensive and inefficient and it is better to compute local distances within space to estimate the global distances (De Smith, 2005). This can be done using Chamfer matrices.

Variable topography distance transforms
Variable topography distance transforms (VTDT) can be used to find the optimal paths across landscape when this is presented in digital elevation format. VTDT can be used to find shortest distances in cells in 3-D landscape by introducing constraints. If each cell is represented with latitude, longitude and altitude, the height difference makes it possible for the slope between two adjacent cells to be calculated by the algorithm. A VTDT algorithm gives the shortest path by using digital transforms on digital elevation models and introducing constraints. The central function in VTDT algorithm is given Equation 1:

$$S = \frac{(H_{i+m,j+n} - H_{i,j})}{c_{m,n}} \tag{1}$$

where s is slope, , $c_{m,n}$ is the distance from origin to the point (i, j), and s_{max} is maximum allowable slope.

The digital elevation model is a 2-D matrix where every element H_{ij} represents the height in the corresponding surface location (i,j). The gradient and slope constraints are implemented in variable topography distance transform by the condition:

$$\begin{aligned} &\text{If} && (H_{i+m,j+n} - H_{ij} < \Delta H_c) \\ &\text{and} && s < s_{max} \\ &\text{then} && d_{i,j} = \min(d_{i+m,j+n} + c_{m,n}, d_{i,j}) \\ &\text{else} && d_{i,j} = d_{j,i} \end{aligned} \tag{2}$$

where the height ($H_{i+m,j+n}$) and slope s are calculated from the altitudes of the cells in question from the digital elevation map (DEM). The critical values of height difference (ΔH_c) and slope s_{max} are user defined (Jónsson, 2014).

2.2 Pressure drop

It is important to ensure that the pressure drop in transmission pipelines is minimised. High pressure drops in the steam pipelines can cause loss of power generation if it causes the steam to get to the power plant at pressures below the design turbine inlet pressure. In the brine pipelines, high pressure drops can lead to pressure of brine going below saturation pressures. This would lead to the brine boiling and causing undesirable flow regimes.

Single-phase pressure drop
Single-phase pressure drop is fairly easy to estimate with equations available for it. The total pressure drop in single phase consists of frictional and static pressure drop. The static pressure loss will be the difference in elevation between the end and start of the pipe. Friction pressure loss will be a function of fluid velocity, pipe internal diameter, pipe roughness and Reynolds number. Single-phase pressure drop per unit length is calculated from the Darcy-Weisbach equation given in Equation 3:

$$\frac{dp}{L} = f\frac{\rho v^2}{2D_i} \tag{3}$$

where dp is pressure drop (Pa); L is length of pipe (m); f is friction factor; ρ is the fluid density (kg/m^3); v is flow velocity (m/s); and D_i is the pipe internal diameter (m).

Equation 1 above can also be rewritten in head loss terms as Equation 4 or 5:

$$dp = \rho g dh \tag{4}$$

$$\frac{dh}{L} = f\frac{v^2}{2gD_i} \tag{5}$$

where dh is head loss

Reynolds number Re is then calculated using Equation 6:

$$Re = \frac{\rho v D_i}{\mu} \tag{6}$$

The friction factor f can then be calculated from the Colebrook-White equation (Equation 7) or approximated from the Moody diagram:

$$\frac{1}{\sqrt{f}} = -2log_{10}\left(\frac{\in}{3.7D} + \frac{2.51}{Re\sqrt{f}}\right) \tag{7}$$

where $\in$ is pipe roughness height (m).

Two-phase pressure drop

Two-phase pressure drop consists of frictional, elevation change (gravitational) and momentum change terms. The main parameters extensively used are mass velocity and void fraction. Generally, two-phase flow is modelled as single phase but with a correction factor. The correction factors will vary depending on the flow regime present. The models used in pressure drop estimation can be classified as either homogeneous or separated. Homogenous ones assume that the liquid and gas phases flow at a common velocity while the separated ones assume these two phase flow at different velocities. In both models the void fraction will need to be calculated. This refers to the cross-section of the pipe occupied by the gas phase as a fraction of the total pipe cross-sectional area. Pressure drop per unit length in two phase flow can be represented by the basic conservation of momentum equation (Equation 8) as:

$$\left(\frac{dp}{dz}\right) = \left(\frac{dp}{dz}\right)_f + \left(\frac{dp}{dz}\right)_a + \left(\frac{dp}{dz}\right)_g \tag{8}$$

where $\left(\frac{dp}{dz}\right)$ = total pressure drop per unit length; $\left(\frac{dp}{dz}\right)_f$ = pressure drop per unit length due to friction; $\left(\frac{dp}{dz}\right)_a$ = pressure drop per unit length due to acceleration; $\left(\frac{dp}{dz}\right)_g$ = pressure drop per unit length due to elevation (gravity).

The equation of the individual components can be defined by means of momentum balance. The equation can be rewritten as Equation 9:

$$\frac{dp}{dz} = \frac{\tau P}{A} + m^2\frac{d}{dz}\left(\frac{(1-x)^2}{\rho_L(1-\alpha)} + \frac{x^2}{\rho_G\alpha}\right) + g\rho_{TP}sin\theta \tag{9}$$

where τ is wall shear stress (N/m^2); P is channel periphery (m); A is channel cross-sectional area (m^2); m is mass flow rate (kg/s); x is steam fraction; α is void fraction; ρ_L is liquid density (kg/m^3); ρ_G is vapour density (kg/m^3); ρ_{TP} is two-phase density (kg/m^3); θ is angle between pipe axis and horizontal; and g is gravitational acceleration (m/s^2).

The two-phase density ρ_{TP} and dynamic viscosity μ_{TP} are defined as the average density or dynamic viscosity between the two phases (liquid and gas), and is dependent on the model selected (Freeston, 1982). For the homogenous flow model it will be defined by the Equation 10 and 11:

$$\frac{1}{\rho_{TP}} = \frac{x}{\rho_G} + \frac{1-x}{\rho_L} \tag{10}$$

$$\frac{1}{\mu_{TP}} = \frac{x}{\mu_G} + \frac{1-x}{\mu_L} \tag{11}$$

where μ_G is gas phase dynamic viscosity (kg/ms); and μ_L is liquid phase dynamic viscosity (kg/ms)

For the separated flow model it will be defined by Equation 12:

$$\rho_{TP} = \alpha\rho_G + (1-\alpha)\rho_L \tag{12}$$

From Equations 10-12 above, a void fraction α correlation is needed. Harrison modified the correlation by Butterworth (Freeston, 1982) to obtain Equation 13:

$$\alpha = \frac{1}{1 + (\frac{1-x}{x})^{0.8} (\frac{\rho_G}{\rho_L})^{0.515}} \tag{13}$$

Generally, the frictional pressure drop contributes to most of the total pressure drop but the calculation can be inaccurate for oversized or undersized pipes. The frictional pressure drop is usually referred to as that of a single phase flowing under certain hydrothermal conditions. The term *Two-Phase Multiplier* is the relating factor and presents two-phase frictional pressure drop as that of the gas or liquid phase flowing alone. Frictional multipliers for gas and liquid are defined by Equations 14 and 15:

$$\emptyset_G^2 = \frac{(dp/dz)_{TP}}{(dp/dz)_{fG}} \tag{14}$$

$$\emptyset_L^2 = \frac{(dp/dz)_{TP}}{(dp/dz)_{fL}} \tag{15}$$

Friction multiplier use approach is used in the *Lockhart-Martinelli* correlation as discussed by Hewitt (1982). The multiplier is obtained by defining the Lockhart-Martinelli parameter *X* (Equation 16) also referred to as the pressure drop ratio:

$$X^2 = \frac{(dp/dz)_{fL}}{(dp/dz)_{fG}} = (\frac{1-x}{x})^{1.8} (\frac{\rho_G}{\rho_L}) (\frac{\mu_G}{\mu_L})^{0.2} \tag{16}$$

From the standard Darcy-Weisbach pressure drop equation (Equation 17), and using the gas phase, single-phase pressure drop can now be rewritten as:

$$\left(\frac{dp}{dz}\right)_G = f \frac{L}{2D_i} \rho_G v_G^2 \tag{17}$$

and the resulting two phase pressure drop will then be represented by Equation 18:

$$dp_{TP} = \emptyset^2 f \frac{L}{2D_i} \rho_G v_G^2 \tag{18}$$

where ρ_G is gas density (kg/m^3); v_G is gas flow velocity if flowing alone in pipe (m/s); D_i is pipe internal diameter (m); dp_{TP} is two-phase pressure drop (Pa), L is effective pipe length (m); f is friction factor; and $\emptyset$ is two-phase multiplier

Steam velocity can then be calculated from Equation 19:

$$v_G = \frac{4mx}{\rho_G \pi D_i^2} \tag{19}$$

The two-phase pressure drop will then be also rewritten as Equation 20:

$$dp_{TP} = \frac{8\emptyset^2 Lfmx}{\pi^2 D_i^5 \rho_G} \quad (20)$$

Friction factor f is a function of the Reynolds number Re and pipe roughness $\in$. Reynolds number can then be calculated for the gas phase from Equation 21:

$$Re_G = \frac{\rho_G v_G D_i}{\mu_G} \quad (21)$$

Similarly as in single-phase pressure drop, the friction factor f can then be calculated from the Colebrook-White equation (Equation 7) or approximated from the Moody diagram. A simplified explicit equation (Equation 22) may also be used:

$$f = \frac{0.25}{\left(log_{10}\left(\frac{\in}{3.7D_i} + \frac{5.74}{Re^{0.9}}\right)\right)^2} \quad (22)$$

Friedel method uses a two-phase multiplier similar to the *Lockhart-Martinelli* method to convert the liquid phase pressure drop into two-phase pressure drop. This method first defines two-phase density as in Equation 23:

$$\rho_{TP} = \left(\frac{1}{\rho_G} + \frac{1-x}{\rho_L}\right)^{-1} \quad (23)$$

The two-phase multiplier is then determined using the Weber number We, Froude number Fr and constants *E, F* and *H,* which can be calculated using inputs from saturated water and steam properties and Equations 24 and 25:

$$Fr = \frac{m^2}{gD_i\rho_{TP}^2} \quad (24)$$

$$We = \frac{m^2 D_i}{\rho_{TP}\sigma} \quad (25)$$

where σ is surface tension (kg s^{-2}).

The constants *E, F* and *H* can be calculated from Equations 26-28:

$$E = (1-x)^2 + x^2\frac{\rho_L f_{GX}}{\rho_G f_{LX}} \quad (26)$$

$$F = x^{0.78}(1-x)^{0.24} \quad (27)$$

$$H = \left(\frac{\rho_L}{\rho_G}\right)^{0.91}\left(\frac{\mu_G}{\mu_L}\right)^{0.19}\left(1-\frac{\mu_G}{\mu_L}\right)^{0.7} \quad (28)$$

where f_{GX} is the friction factor for mass flux with steam properties and f_{LX} is the friction factor for mass flux with liquid properties.

The two-phase multiplier is then calculated from Equation 29:

$$\emptyset_L^2 = E + \frac{3.24FH}{Fr^{0.045}We^{0.035}} \quad (29)$$

The two-phase pressure drop can then be calculated using the multiplier and the liquid phase pressure drop using Equation 30:

$$dp_{TP} = \emptyset_L^2 \frac{2f_{LX}(m/A)^2}{\rho_L D_i} \quad (30)$$

Recommendations from Hewitt (1982) concerning the correlations to be used are as follows:

1. For $\mu_L/\mu_G < 1000$, Friedel correlation should be used;
2. For $\mu_L/\mu_G > 1000$, and $m > 100$, Chisholm correlation should be used; and
3. For $\mu_L/\mu_G > 1000$, and $m < 100$, Martinelli correlation should be used.

Pressure loss in bends and fittings
Pressure drop in pipe bends and fittings can be done by use of the equivalent length procedure. The pipeline, discussed here, has a similar number of bends as the ones discussed in Ouma (1992). An additional 15% of the total pipe length is recommended based on earlier works by VGK Consulting Engineers of Iceland. This caters for losses from bends and fittings fairly accurately.

2.3 Pipe mechanical design

Pipe thickness
Consideration of nominal thickness of pipe is dependent on the operating pressure of the system. Pipe thickness is selected so that the pipe is able to resist the design pressure over its lifetime. ASME 31.1 power piping design codes (ASME, 2007) provide the criteria of pipe thickness selection given by Equation 31:

$$t_n \geq t_m = \frac{pD_o}{2(SE + py)} + A_C \tag{31}$$

where t_n is nominal pipe thickness (m); t_m is required pipe thickness (m); p is design pressure (Pa); D_o is outer pipe diameter (m); S is allowable stress (MPa); E is welding factor (dimensionless); y is temperature dependent coefficient; A_C is corrosion allowance (m).

For this system, wellhead pressure will be the highest pressure in the system. A margin can be added to the wellhead pressure and used as the maximum pressure the system would be subject to over its operating life.

Stress analysis
Loads acting on a pipe can be due to internal and external pressure, temperature, pipe material and contents conveyed, cladding material, fittings like valves, environmental effects like wind and snow and sudden transient effects like water hammer. Usually, the total loads would be a combination of a number of these loads. Loads acting on a pipe can be classified as either sustained or occasional loads.

(i) Sustained load criteria
The condition that must be fulfilled for the sustained loads acting on a pipe is defined by Equation 32:

$$\frac{pD_o}{4t_n} + 0.75i\left(\frac{M_A}{Z}\right) \leq S_h \tag{32}$$

where i is stress intensity factor ($0.75i \geq 1.0$); M_A is sustained bending moment, Z is section modulus; and S_h is allowable stress during operation (hot).

The section modulus Z is calculated from Equation 33:

$$Z = \frac{\pi}{32}\left(\frac{D_o^4 - D_i^4}{D_o}\right) \tag{33}$$

Vertical sustained loads
Vertical sustained loading is a combination of the weight of the pipe, weight of the insulation and weight of cladding material per unit pipe length. This can be calculated from Equation 34:

$$q_{sv} = q_p + q_e + q_c \quad (34)$$

where q_{sv} is vertical sustained load; q_p is weight of pipe; q_e is weight of insulation material; q_c is weight of cladding material.

The individual weights can be calculated from the Equations 35-37:

$$q_p = \frac{\pi}{4} g\rho_s(D_o^2 - D_i^2) \quad (35)$$

$$q_e = \frac{\pi}{4} g\rho_e(D_e^2 - D_o^2) \quad (36)$$

$$q_c = \frac{\pi}{4} g\rho_c(D_c^2 - D_e^2) \quad (37)$$

where ρ_s is density of steel; ρ_e is density of insulation material; ρ_s is density of cladding material; D_e is diameter of insulation; and D_c is diameter of cladding.

(ii) Occasional loads

The condition that must be fulfilled for the occasional loads acting on a pipe is defined by Equation 38:

$$\frac{pD_o}{4t_n} + 0.75i\left(\frac{M_A}{Z}\right) + 0.75i\left(\frac{M_B}{Z}\right) \leq kS_h \quad (38)$$

where M_B is the occasional bending moment; k is the load factor dependent on duration of operation time; k = 1.15 if loading is less that 10% of operational time; k = 1.2 if loading is less that 1% of operational time; k = 1.0 otherwise.

Vertical occasional loads

Vertical occasional load is a combination of the weight of the transported medium, snow load and seismic load. It is calculated from Equation 39.

$$q_{ov} = q_v + q_s + q_{ev} \quad (39)$$

where q_{ov} is vertical occasional load; q_v is weight of pipe contents; q_s is snow load; and q_{ev} is vertical seismic load.

The individual weights can be calculated from the Equations 40-42:

$$q_v = \frac{\pi}{4} g\rho_v D_i^2 \quad (40)$$

$$q_s = 0.2sD_c \quad (41)$$

$$q_{ev} = 0.5eq_g \quad (42)$$

where ρ_v is density of medium in pipe; s is snow factor; e is seismic factor; q_g is total load subject to gravity (sum of weight of pipe, medium, lagging and cladding).

Hence:

$$q_g = q_p + q_v + q_e + q_c \quad (43)$$

Horizontal occasional loads

Horizontal occasional loads refer to the maximum load calculated between the wind load, q_w and the horizontal seismic load, q_{eh}:

$$q_w = C\rho_w D_c \quad (44)$$

$$\rho_w = \frac{v_w}{1.6} \quad (45)$$

$$q_{eh} = eq_g \tag{46}$$

where v_w is wind speed (m/s).

Horizontal occasional loads can therefore be determined from Equation 47:

$$q_{oh} = \max(q_w, q_{eh}) \tag{47}$$

Bending moments
The pipeline behaves like a beam and the sustained and occasional bending moments can be calculated from Equations 48 and 49:

$$M_A = \frac{q_{sv}L_S^2}{8} \tag{48}$$

$$M_B = \sqrt{(q_{ov}^2 + q_{oh}^2)}\,\frac{L_S^2}{8} \tag{49}$$

where L_S is the length between supports (m).

Length between supports
Length between supports is selected to meet the conditions of Equation 50:

$$L_S^2 \leq \frac{\left(kS_h - \frac{pD_o}{4t_n}\right)\{\frac{\pi}{4}(D_o^4 - D_i^4)\}}{D_o(0.75i)\left(q_{sv} + \sqrt{q_{ov}^2 + q_{oh}^2}\right)} \tag{50}$$

Deflection
Pipe deflection can then be calculated from Equations 51 and 52:

$$\delta = \frac{2.07qL^3}{384EI} \tag{51}$$

and

$$I = \frac{\pi(D_o^4 - D_i^4)}{64} \tag{52}$$

where δ is maximum allowable deflection; E is Young's modulus; and I is the moment of inertia of the pipe cross-section.

2.4 Separator design considerations

Separator placement
Separator location is very crucial in the design of a steam gathering system. The following are critical factors that need to be taken into account when placing separators.

(i) Elevation
Separator or separating station elevation in respect to production and reinjection wells must be considered when siting separators. It is always desirable that separators are placed at a low elevation compared to the production wells to avoid going into undesirable flow regimes by flowing two-phase fluid uphill. The separators should also be placed at a higher elevation than the reinjection wells to allow reinjection brine to flow freely by gravity into the reinjection points and eliminate the need to use pumps that would be otherwise increase the cost of installation and operation.

(ii) Location

Placement of separators close to the wells results in low pressure drops in two-phase pipelines while having separators close to the power plant would lead to high pressure drops in these two-phase pipelines. Both of these scenarios may be beneficial based on the reservoir pressure of the resource being utilised. Optimal separator location is desirable for separators that can handle fluid from a number of wells (Onyango, 2015).

Separator dimensions and wall thickness

Geothermal separators are generally classified as either horizontal or vertical (DiPippo, 2016). Vertical separators use the principle of centrifugal or cyclonic separation. The centrifugal force is generated using a tangential or spiral inlet to the cyclone. As the fluid rotates, the water with a higher density will tend to flow to the walls of the vessels and downwards while the steam with a much lower density will tend to flow inwards and upwards. Horizontal separators on the other hand are based on a gravitational separation process. The mixture will enter from the top and travel horizontally while flashing occurs. The design is to ensure the mixture velocity is sufficiently lowered to give the water particles enough time to settle to the bottom before steam leaves from the top on separators. The technology was in use earlier in the nuclear industry. Vertical separators are the most widely used in the world due to the simplicity of their design and construction.

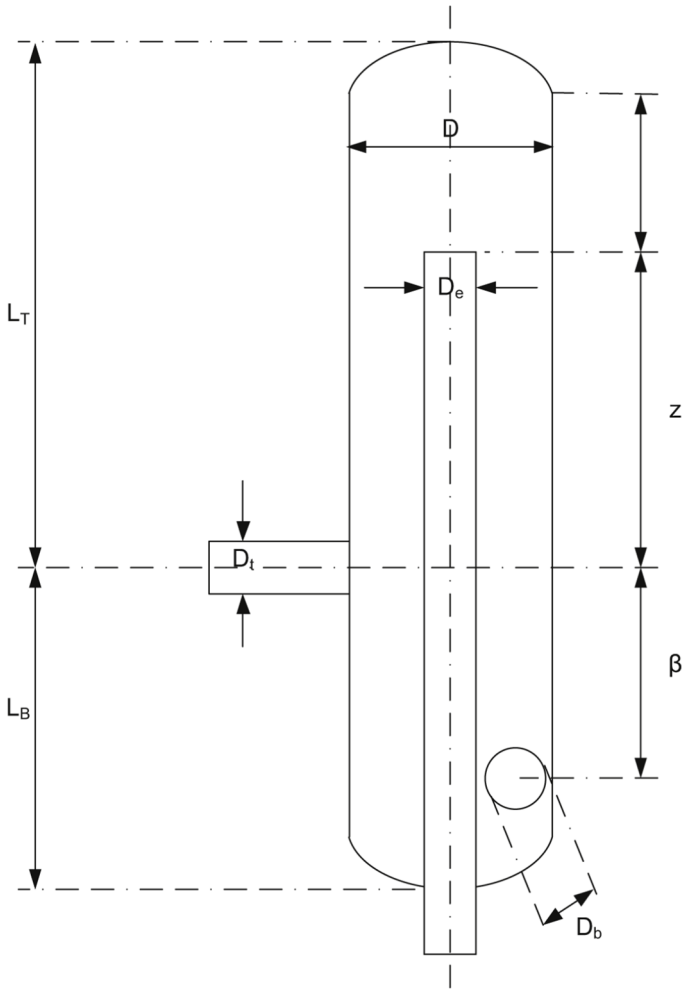

FIGURE 6: Vertical separator dimensions (Lazalde-Crabtree, 1984)

Vertical separator dimensions

The key principle in vertical separators is to generate a vortex that will push the liquid to the vessel walls and concentrate the steam in the centre. Bangma (1961) and Lazalde-Crabtree (1984) methods can be used to design the dimensions of the vertical cyclone separator (Figure 6). Inlet cross-sectional area, A_i and diameter, D_t are calculated using Equations 53 and 54, respectively:

$$A_i = \frac{Q_{vs}}{v_t} \tag{53}$$

$$D_t = \left(\frac{4A}{\pi}\right)^{0.5} \tag{54}$$

where A_i is internal cross-sectional area of inlet; Q_{vs} is volumetric steam flow; D_t is inlet pipe diameter; and v_t is two-phase inlet steam velocity.

The two-phase inlet diameter D_t is calculated from the equations above, and the rest of the vessel dimension is given in terms of D_t. Purnanto et al. (2012) summarised vertical separator design guidelines from earlier works (Table 3) for the separator dimensions in terms of D_t.

TABLE 3: Vertical separator dimensions (Purnanto et al., 2012)

Parameter	Bangma	Lazalde-Crabtree	Spiral inlet
D	$3D_t$	$3.3D_t$	$2.95D_t$
D_e	$0.8D_t$	D_t	D_t
D_b	D_t	D_t	$0.7D_t$
α	$3.25D_t$	$0.15D_t$	$0.28D_t$
β	$3D_t$	$3.5D_t$	$3.2D_t$
Z	$3D_t$	$5.5D_t$	$5.8D_t$
L_T	$7D_t$	$6.475D_t$	$6.8D_t$
L_B	$4.5D_t$	$4.975D_t$	$4.9D_t$

Additional recommendation for fluid velocity in the separator is provided by DiPippo (2016) as summarised in Table 4.

TABLE 4: Recommended cyclone inlet and steam velocities (DiPippo, 2016)

Parameter	Velocity
Maximum steady velocity at two-phase inlet pipe	45 m/s
Recommended range of steady velocity at two-phase inlet pipe	25–40 m/s
Maximum upward annular steam velocity inside cyclone	4.5 m/s
Recommended range of upward annular steam velocity inside cyclone	2.5–4.0 m/s

Separator wall thickness

Separator wall thickness is determined using the same equations used to determine pipe wall thickness. The thickness of the walls should be sufficient to resist pressure of the vessel in working conditions. Equation 55 is used to calculate minimum wall thickness t (ASME, 2007):

$$t = \frac{pD}{2SE - 0.2p} + A_C \tag{55}$$

where t is minimum wall thickness (m); p is separator design pressure (mPa); D is separator outside diameter (m); S is material allowable stress (MPa); E is welding factor and A_C corrosion allowance (m).

3. WELL OW-906 DESIGN AND RESULTS

3.1 General information

Ambient conditions

Table 5 below gives a summary of the weather and geographical conditions that will be used in this work.

TABLE 5: Weather and geographical conditions for Olkaria Domes field

Average wet bulb temperature (°C)	35
Average dry bulb temperature (°C)	17
Atmospheric pressure (bara)	0.8
Relative humidity maximum (%)	70
Average annual rainfall (mm)	700
Wind speed maximum (m/s)	36
Wind shape facor	0.6
Seismic factors (UB, Zone 3)	0.16

Well location
Well OW-906 is situated on the eastern side of the Olkaria Domes field. Table 6 below shows the coordinates of the well. The well is a directional well drilled to a depth of 2200 meters.

TABLE 6: Well OW-906 cordinates

Northing	9899827
Easting	201803
Elevation (m a.s.l.)	1975

The well was drilled between July 2012 and January 2013 as a production well for the then proposed Olkaria IV power plant.

Well completion test data
Injection temperature profile for the well shows permeability down to about 1600 m. Below this depth, conductive heating controls the well, as indicated on the heat up profiles in Figure 7.

The major feed zone was observed to be at a depth of about 1500 m. Pressure injection test showed minimal pressure build-up while injecting water at the highest pump rate of 1900 L/min. (Figure 8).

The well has an injectivity index of 434.3 Lpm/bar (Figure 9). This is a relatively high injectivity index, in comparison to most wells in the vicinity and in the Olkaria Domes field. The well also has a high permeability. This is supported by the high injectivity index and the minimal pressure build up during the injection tests.

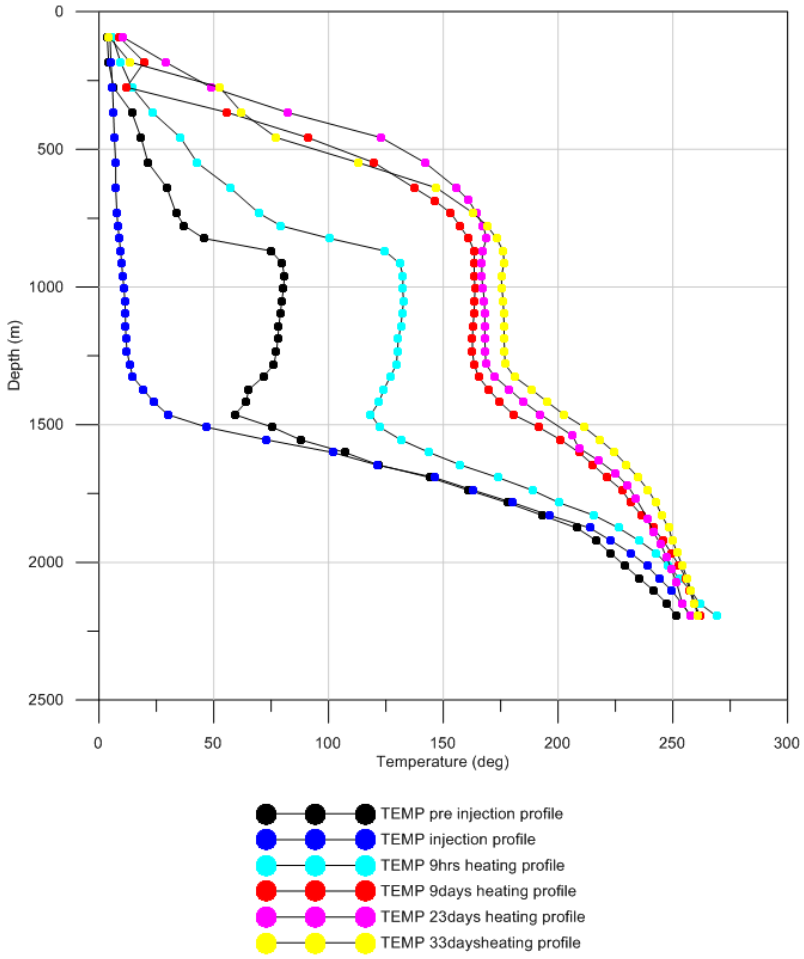

FIGURE 7: Well OW-906 temperature profiles (KenGen, 2013)

Well discharge test data
The well discharge tests were carried out for four days in April 2013 and two days in June 2013. The tests were, however, interrupted to allow for the connection of the reinjection pipeline for the well. The well was sacrificed to be a reinjection well due to the observed high brine outputs of the Olkaria Domes field and therefore more reinjection capacity was needed. This however changed after commissioning of the Olkaria Domes steam field where it was established that the reinjection capacity was actually excessive. In addition to the steam field pressure that was raised to 11 bar, which reduced the reserve steam margin, this justified the reconnection of the well for production. Well discharge test data in Table 7 below shows computed well output using lip pressure pipe of diameter 0.2 m. The data indicates that the well is a fairly good producer.

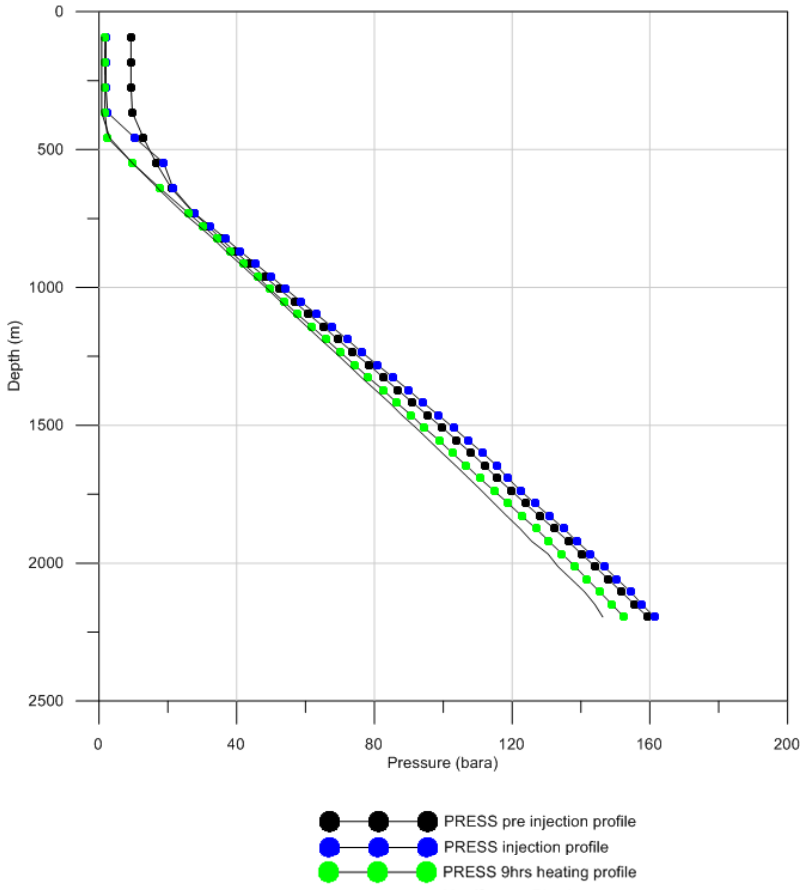

FIGURE 8: Well OW-906 pressure profiles (KenGen, 2013)

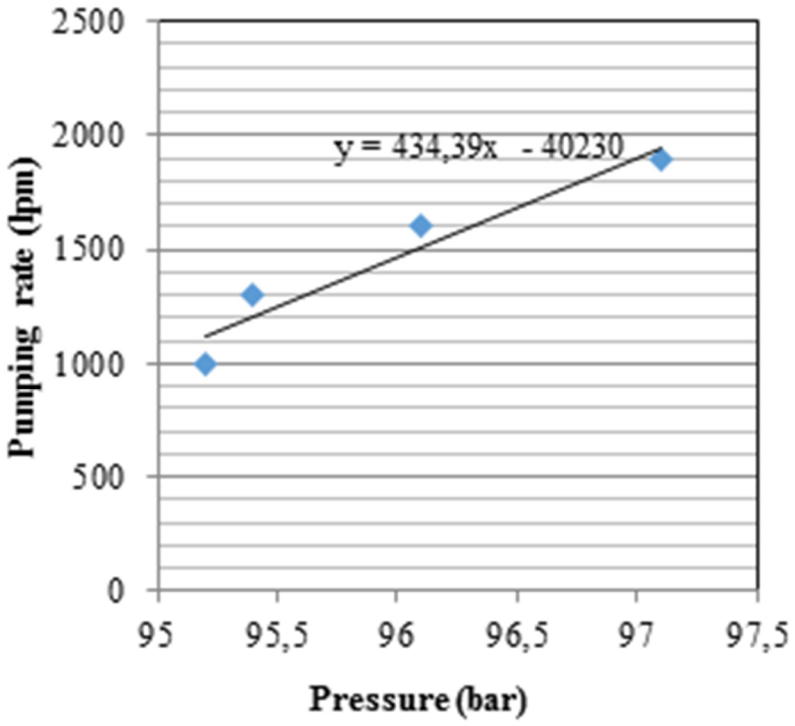

FIGURE 9: Well OW-906 injectivity index (KenGen, 2013)

The discharge tests were carried out for a very short period and the data obtained cannot be relied upon. For this work, fluid enthalpy of nearby wells was used to estimate fluid properties for 13.0 bar-a wellhead pressure as indicated in Table 8 below. The total mass flow was assumed to remain the same and was maintained at 44 kg/s. Selected fluid enthalpy used was 1350 kJ/kg and Engineering Equation Solver (EES) was used to calculate steam flow and water flow at a separation pressure of 12 bar-a. The results are as indicated in Table 8. This is the data that will be used in the design presented here.

TABLE 7: Well OW-906 discharge data with 200 mm lip pipe

Date	Well pressure (bara)	Total mass (kg/s)	Enthalpy (kJ/kg)	Water flow (kg/s)	Steam flow (kg/s)	Power output (MW)
28 Apr 13	7.3	48.2	1003	35.7	8.3	4.2
28 Apr 13	7.3	47.9	1009	35.3	8.4	4.2
29 Apr 13	7.3	46.6	1035	33.8	8.7	4.4
29 Apr 13	7.3	46.6	1035	33.8	8.7	4.4
04 Jun 13	7.5	44.1	1125	30.2	10.2	5.1
05 Jun 13	7.5	44.1	1125	30.3	10.2	5.1

TABLE 8: Well OW-906 recalculated discharge data for design

Well pressure (bar-a)	Separator pressure (bar-a)	Total mass (kg/s)	Enthalpy (kJ/kg)	Water flow (kg/s)	Steam flow (kg/s)
13.0	12.0	44.0	1350	32.0	12.0

3.2 Pipeline route selection

Pipe route selected is carried out using variable topology distance transform (VTDT) with the Olkaria IV digital elevation matrix (DEM) as the input file. The maximum height difference was set at 0.1 and the maximum slope restricted to 0.025 for the two-phase pipeline. There are no constraints in this area. Figure 10 below shows the Olkaria IV DEM with the existing separation stations. Five options will initially be considered, i.e. flow of two-phase fluid to the four existing separators and creation of an optimised separator position near the well.

The selection of the two-phase pipeline route and the brine reinjection pipeline route is done based on the optimised separator location. Two-phase and steam pipelines will be designed based on the selected existing separator stations or an optimised alternative location between the well and the closest main steam pipeline. The reinjection pipeline is limited by the fact that existing reinjection wells are to be used. Table 9 shows the locations of the existing separator stations.

Figure 10 shows the digital elevation matrix for Olkaria IV showing well OW-906 and the four existing separator stations. Results of the variable topology distance transform are shown in Figures 11 and 12.

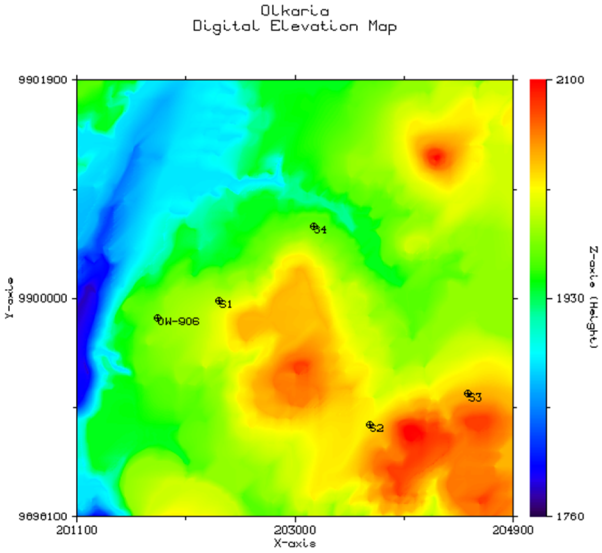

FIGURE 10: Olkaria IV Digital Elevation Matrix showing well OW-906 and existing separators

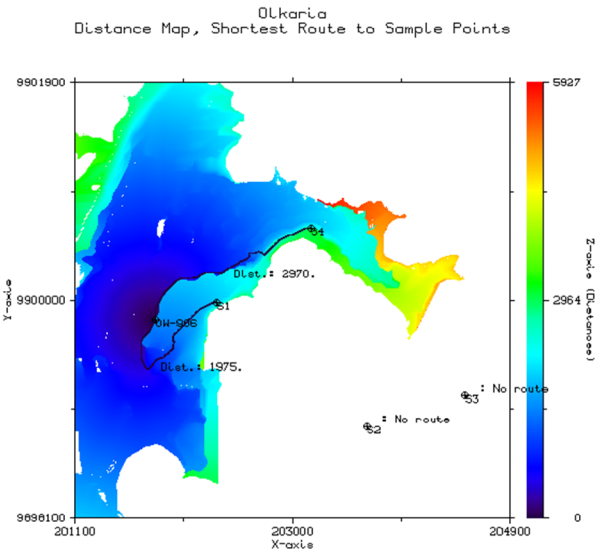

FIGURE 11: Two-phase pipelines with distances from OW-906 to separator stations SD1 and SD4

TABLE 9: Coordinates of existing separator stations

Station	Northing	Easting	Elevation
SD1	9899980	202340	1985
SD2	9898900	203650	2010
SD3	9899170	204510	2029
SD4	9900630	203160	1960

TABLE 10: VTDT results for distances from OW-906 to separator stations SD1, SD4 and SD5

Pipeline route	Fluid type	Distance (m)
OW-906 to SD1	Two-phase	1975
OW-906 to SD4	Two-phase	2970
OW-906 to SD5	Two-phase	100

TABLE 11: Coordinates of existing brine reinjection wells

Reinjection well	Northing	Easting	Elevation (m a.s.l.)
OW-901	9900842	201857	1891
OW-902	9899012	201681	1951
OW-906A	9899916	201724	1964
OW-911	9898315	202736	1979
OW-911A	9898287	202725	1979
OW-913A	9899117	202341	1980

From Figure 11, separator stations SD2 and SD3 are located at much higher elevations than the production well OW-906 and are therefore not accessible for two-phase flow from this well. The separator stations accessible to this well are SD1 and SD4. The results of the distances to these two accessible separators using VTDT is summarised in Table 10. VTDT results also indicate the optimal separator positioning is within the OW-906 well pad as shown by the black dot on Figure 12 below. This new separator station is designated as SD5 and its distance from the well is also shown in Table 10. VTDT was also used to estimate the distances to all the reinjection wells to determine the nearest reinjection well accessible to the brine from the new separator station SD5.

As Table 11 shows, all the reinjection wells are below the well pad OW-906 and are therefore available for free flow of brine by gravity. However, the well to be used is selected based on the shortest distance from the separator station. Figures 13 indicates the results of VTDT for position of the new separator station SD5 and all the reinjection wells. Figure 14 shows the optimal pipeline routes and distances from SD5 to these reinjection wells from SD5.Results of the distances of the reinjection wells are summarised in Table 12.

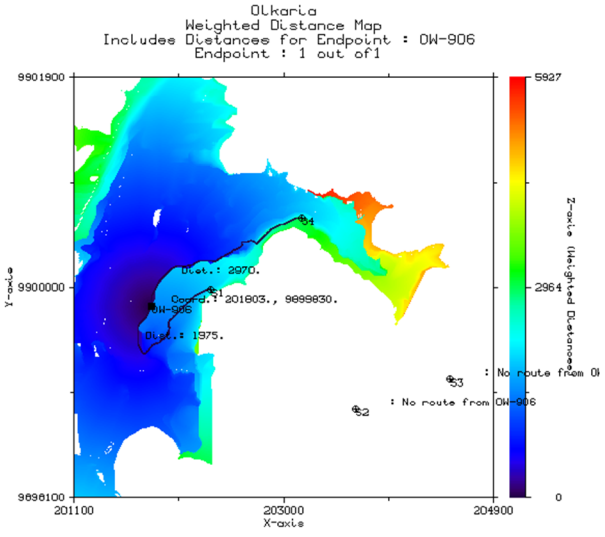

FIGURE 12: Two-phase pipelines with distances from OW-906 to separator stations SD1 and SD4 showing optimal separator location (black dot)

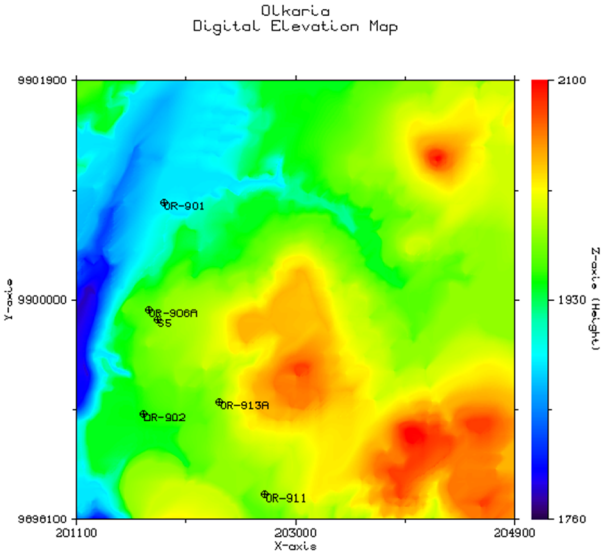

FIGURE 13: Olkaria IV DEM with new separator station SD5 and all the reinjection wells

From the VTDT results of the two-phase pipelines from well OW-906 to separator stations SD1 and SD4, only the SD4 option will be considered further. Both pipelines are fairly long for two-phase flow due to the high associated pressure drops but SD1 provided an additional problem of having to flow two-phase uphill and this is undesirable especially for long distances. The well to be used for the reinjection is selected based purely on the length of the pipeline. The shortest distance is to well OW-906A.

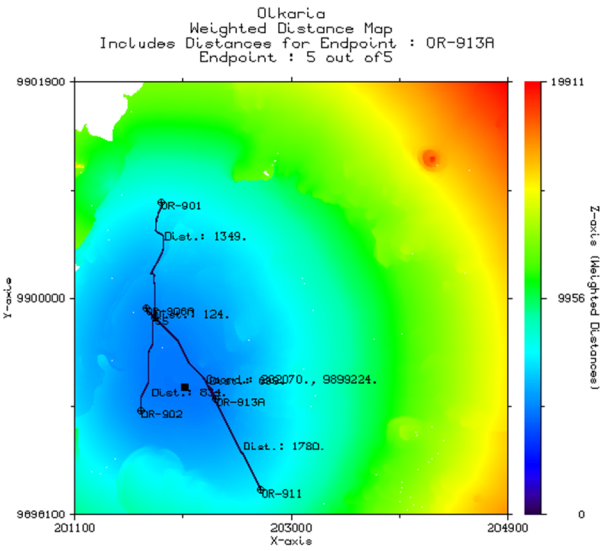

FIGURE 14: Olkaria IV DEM with new separator station SD5 and all the reinjection pipeline routes and distances from the separator

For the steam pipelines, VTDT is applied to find the distances from separator station SD5 to the nearest main steam pipeline towards the power plant. The closest main steam line is the main steam pipeline from separator station SD1 towards the power plant. Five anchors along this pipe are considered as possible tie-in points for this new pipeline. VTDT is therefore used to establish the shortest optimal path to the nearest anchor. For steam pipelines, the slope is not relevant. Table 13 shows the coordinates of the anchors along this main steam pipeline.

TABLE 12: VTDT results for distances from separator station SD5 to existing reinjection wells

Pipeline route	Fluid type	Distance (m)	Well elevation (m a.s.l.)
SD5 to OW-901	Brine	1349	1892
SD5 to OW-902	Brine	834	1952
SD5 to OW-906A	Brine	124	1964
SD5 to OW-911	Brine	1790	1980
SD5 to OW-911A	Brine	1797	1980
SD5 to OW-913A	Brine	899	1981

Figure 15 indicates the results of VTDT for positions of the nearest anchors on the main steam pipeline near the new separator station SD5. Figure 16 shows the optimal pipeline routes and distances from SD5 to the anchor points on the main steam pipeline near the separator station.

TABLE 13: Coordinates of five anchors on the main steam pipeline considered as new steam pipeline tie-in points

Anchor identity	Northing	Easting	Elevation (m a.s.l.)
A-1	9899939	202123	1980
A-2	9899908	202090	1979
A-3	9899814	201990	1977
A-4	9899629	201900	1968
A-5	9899548	201870	1965

TABLE 14: VTDT results for distances from separator station SD5 to nearest anchor points on main steam pipeline

Pipeline route	Fluid type	Distance (m)
SD5 to A-1	Steam	341
SD5 to A-2	Steam	301
SD5 to A-3	Steam	217
SD5 to A-4	Steam	316
SD5 to A-5	Steam	535

Results of the distances of the anchor points on the main steam pipeline to separator station SD5 are summarised in Table 14.

The two design options to be considered for optimisation and compared in this work are summarised in Table 15 and are the following:

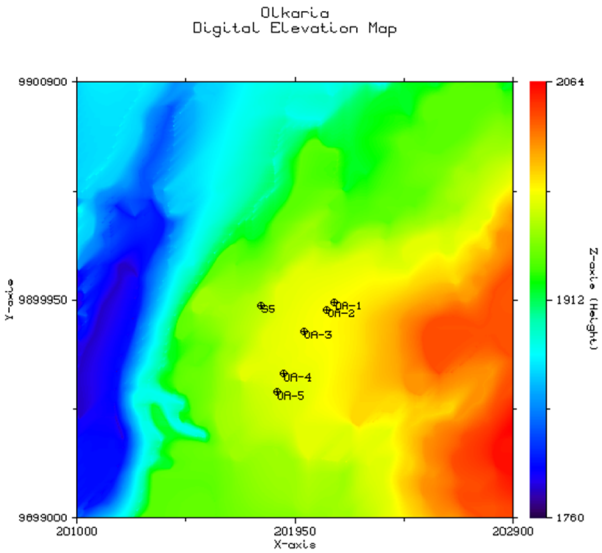

FIGURE 15: Olkaria IV DEM with anchor points on the main steam pipeline near new SD5

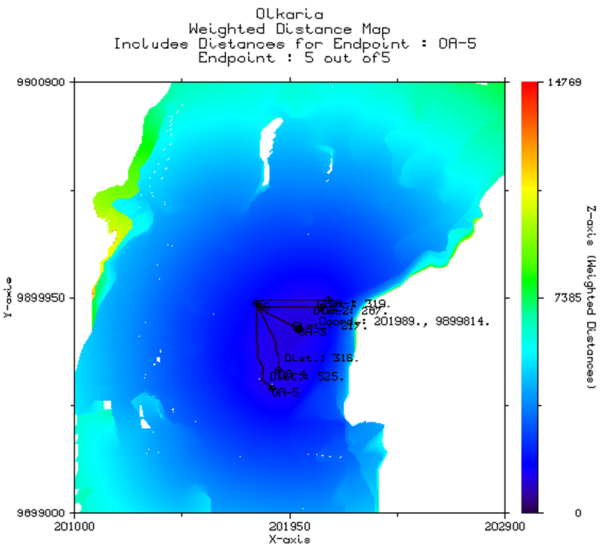

FIGURE 16: Olkaria IV DEM with optimal routes to anchor points on the main steam pipeline near SD5

TABLE 15: Summary of design items for the options to be optimised and compared

Design option	Items
1	1. Design of two-phase pipeline from well OW-906 to existing separator station - SD4 – 2790 m. 2. Assess capacity of brine and steam pipeline to accommodate additional flow.
2	1. Design two-phase pipeline to the new separator station SD5 located on the OW-906 wellpad – 100 m. 2. Design separator station SD5. 3. Design steam pipeline from SD5 to nearest anchor on main steam pipeline – 187 m. 4. Assess capacity of brine and steam pipeline to accommodate additional flow.

Design option 1: Flowing of two-phase fluid downhill to existing separator SD4. In this case the pipe route design will be done for two-phase flow to SD4. Brine from SD4 is already connected to flow to reinjection well OW-901. Brine and steam pipelines will be assessed to ensure they have additional capacity to accommodate the additional flow.

Design option 2: Flowing of two-phase fluid to a new optimally located separator SD5: In this case the pipe route design will be done for two-phase flow to SD5. Brine reinjection pipeline will be designed to connect to the main brine reinjection pipeline to the nearest reinjection well, OW-906A. Steam pipeline will then be optimally routed and designed to connect to the nearest anchor point along the nearest main steam pipeline.

3.3 Pressure drop and diameter selection

Pressure drop calculations have been carried out using the equations outlined in the previous chapter. All the calculations are calculated for unit pipe lengths. Two-phase pressure drop is calculated using the correlations discussed and the highest value used in this design. Steam and brine pressure drops are calculated using single-phase pressure drop equations.

3.3.1 Two-phase pressure drop

The two-phase pressure drop was carried out using the Friedel method (Appendix I). This method was selected based on the recommendations of Hewitt (1982) where the Friedel method is recommended when μ_L/μ_G is less than 1000. For this well, $\mu_L/\mu_G = 9.37$. Wellhead and separator pressure are set to 1.3 and 1.2 MPa, respectively. Diameter selected is the one that gives pressure drop values below the minimum allowable pressure drop.

Maximum allowable pressure drop is 0.1 MPa
Selected two-phase pipe diameter for Option 1 is DN800
Selected two-phase pipe diameter for Option 2 is DN500

3.3.2 Single-phase pressure drop

Steam
There was no steam pipe selection required for Option 1 because this option will use the existing pipeline from separator station DS4. For option 2, the steam pipeline was selected based on a steam velocity of 30 m/s (Appendix I). Pressure drop in this case was minimal and steam velocity was the key guiding factor in pipe size selection.

Selected steam pipe diameter for Option 2 is DN300

Brine
Brine pipeline is not considered in this work because there is an existing brine pipeline connected to the nearest reinjection well OW-906A with a 70 kg/s capacity to accommodate brine from well OW-906. The well selection is, however, done using VTDT based on distance from the new separator.

3.4 Pipe wall thickness

Pipe wall thickness was calculated using Equation 31 using Excel (Appendix II). The pipe thickness was then selected from nominal thickness tables (Appendix V). For the two-phase and steam pipelines, the design pressure used was 2 MPa corresponding to Class 150.

Calculated minimum thickness for the two-phase pipeline for Option 1 is 11.62 mm;
Selected nominal thickness for Option 1 is 12.7 mm;
Calculated minimum thickness for the two-phase pipeline for Option 2 is 7.14 mm;
Selected nominal thickness for Option 2 is 9.53 mm;
Calculated minimum thickness for the steam pipeline for Option 2 is 5.63 mm;
Selected nominal thickness for Option 2 is 6.35 mm.

3.5 Separator dimensions and wall thickness

Separator dimensions are calculated using Equations 53 and 54 with steam inlet velocity fixed at 30 m/s to calculate inlet diameter D_t. The rest of the separator dimensions were then calculated as a function of D_t. This was done for the spiral inlet option considered the most efficient (Zarrouk and Purnanto, 2014).

Calculated inlet diameter D_t is 288 mm;
Selected inlet diameter of pipe size is DN300.

Table 16 gives the results of the separator dimensions as a function of the selected inlet diameter using the spiral inlet dimensions (see also Appendix III). Pipe thickness was done based on ASME 31.3 design guidelines (Equation 55). Design pressure used was 2 MPa corresponding to Class 150.

Nominal thickness is selected from standard pipe thickness tables (Appendix V).

Calculated separator minimum wall thickness is 10 mm;
Selected nominal separator thickness is 12.7 mm.

TABLE 16: Vertical separator dimensions based on Spiral inlet option

Parameter	Spiral inlet	Dimensions (m)
D	$2.95D_t$	0.9
D_e	D_t	0.3
D_b	$0.7D_t$	0.2
α	$0.28D_t$	0.08
β	$3.2D_t$	0.96
Z	$5.8D_t$	1.7
L_T	$6.8D_t$	2.0
L_B	$4.9D_t$	1.5

3.6 Design options cost comparison

The two design options are compared using the cost of the piping network. The cost is based on the cost of steel per kg for equivalent pipe total lengths. Volume of steel in each of the options is first calculated using the pipe lengths obtained from the VTDT and the pipe thickness calculated from the mechanical design. Cost of steel per unit length for nominal diameters from Kalinci et al. (2007) was modified using standard world steel prices and nominal thickness of the indicated diameters.

Weight of steel was then calculated using density of steel of 7850 kg/m^3 and the cost represented as cost per kg of steel as tabulated in Table 17.

TABLE 17: Modified pipe cost based on pipe weight
(weight/m for nominal pipe thickness (Tioga, 2014 – Appendix V)

Pipe nominal diameter (m)	Total pipe & installation cost (Kalinci et al.) (USD/m)	Pipe weight for nominal thickness (kg/m)	Calculated pipe cost based on weight (USD/kg)
0.20	80	42.5	1.88
0.25	115	60.3	1.91
0.30	145	73.9	1.96
0.35	185	81.3	2.27
0.40	240	93.3	2.57
0.45	285	105.2	2.71
0.50	345	117.2	2.94
0.55	375	129.1	3.01
0.60	424	141.1	3.10
0.65	522	152.9	3.18
0.70	567	164.4	3.21
0.75	613	176.7	3.25
0.80	658	188.8	3.30
0.85	708	212.6	3.33
0.95	754	217.6	3.36
1.00	799	236.6	3.38
1.05	844	255.6	3.40

The cost of the two options is summarized in Table 18.

TABLE 18: Summary of costs for the two options

Option	Items	Total cost of steel (USD)
1	Two-phase pipeline – DN800 Length – 3415 m Thickness – 12.7 mm	3,335,000
2	1. Two-phase pipeline – DN500 Length – 100 m Thickness – 9.5 mm 2. Steam pipeline – DN300 Length – 6.4 m Thickness – 9.5 mm 3. Separator Outside diameter – 0.9 m Thickness – 12.7 mm	64,000

3.7 Pipe stress analysis

3.7.1 Loads acting on pipe and distance between supports

Vertical sustained loads acting on the selected two-phase pipe are calculated using Equation 34. An Excel sheet was created for this calculation (Appendix IV). Insulation used is calcium silicate and a standard thickness of 30 mm is assumed. Vertical and horizontal occasional loads are calculated using Equations 39 and 47, respectively. Maximum distance between supports is calculated using Equation 50. Table 19 below gives the results of the forces acting on pipe and maximum distance between supports for both the two-phase and steam pipes.

TABLE 19: Results of forces acting on the pipe and maximum distance between supports

Pipeline	Results
Two-phase pipe	Vertical sustained load – 1488.9 N/m Vertical occasional load – 134 N/m Horizontal occasional load – 241.7 N/m Maximum distance between supports – 19.8 m Maximum allowable deflection – 2 mm
Steam pipe	Vertical sustained load – 655.5 N/m Vertical occasional load – 57.4 N/m Horizontal occasional load – 130.6 N/m Maximum distance between supports – 21.1 m Maximum allowable deflection – 2 mm

4. CONCLUSIONS

The preliminary pipe routing selection and design of production pipeline for the make-up well OW-906 to Olkaria IV steam gathering system has been carried out. This work clearly shows that it is important to carry out possible pipeline route surveys to come up with the most optimal pipe route and eventually the most cost effective option. The analysis shows that it is cheaper to build a new separator station designated as SD5 on the well pad of OW-906 and use it to separate fluid from the well, then connect the steam to the nearest main steam pipeline that goes from separator station SD4 through separator station SD1 and towards the power plant. The brine from this new separator station will flow to the

nearest reinjection well OW-906A with no additional design changes since this pipeline has sufficient capacity to accommodate the additional flow. The steam will also be accommodated by the existing steam pipeline from separator stations SD1 and SD4. The cost is estimated based on the cost of steel but there is a huge disparity observed between the two options. For this method to be accurately applied, cost must include factors such as labour, foundation costs and other accessories.

ACKNOWLEDGEMENTS

I would like to express my gratitude to the director of UNU Geothermal Training Programme Mr. Lúdvík S. Georgsson and the entire staff for the support accorded to me during the study period. Special thanks goes to my supervisor Magnús Thór Jónsson for his guidance during the period I undertook this project work. I would also like to thank the staff of Orkustofnun and ISOR for their assistance from time to time on very pertinent issues. I would like to also recognize all my colleagues and lecturers for their various inputs to the success of this study period and to the management of KenGen for according me this chance. Last but not least, I would like to express my deepest appreciation to my wife Blanche and daughter Bianca for their understanding.

REFERENCES

ASME, 2007: *ASME 31.1-2007. Power piping.* American Society of Mechanica Engineers, NY.

Bangma, P., 1961: The development and performance of a steam–water separator for use on geothermal bores. *Proceedings of the UN Conference on New Sources of Energy, Vol. 2, Geothermal Energy Agenda, item II.*

De Smith, M.J., 2005: *Determination of gradient and curvature constrained optimal paths*. London University College, publication, 33 pp.

DiPippo, R., 2016: *Geothermal power plants: Principles, applications, case studies and environmental impact.* Elsevier Ltd., Kidlington, UK, 762 pp.

Freeston, D.H. 1982: *Lectures on geothermal energy developments in New Zealand.* UNU-GTP, Iceland, Report 12, 108 pp.

Hance, C.N., 2005: Factors affecting cost of geothermal power development. *Geothermal Energy Association, publication for the US Department of Energy*, 64 pp.

Henriquez M., J.L., and Aguirre L., L.A., 2011: Piping design: The fundamentals. *Paper presented at Short Course on Geothermal Drilling, Resource Development and Power Plants, organised by UNU-GTP and La-Geo, Santa Tecla, El Salvador*, UNU-GTP SC-12, CD, 14 pp.

Hewitt, G.F., 1982: Flow regimes. In: Hetsroni, G. (ed.), *Handbook of multiphase systems.* Hemisphere Publishing Co, USA, 2.24 – 2.94.

Jónsson, M.Th., 2014: *An approach to optimum route and site selection of steam gathering system for geothermal power plants using multiple weight distance transform*. University of Iceland, Reykjavik, 7 pp.

Kalinci, Y., Hepbasli, A., and Tavman, I., 2008: Determination of optimum pipe diameter along with energetic and exergetic evaluation of geothermal district heating systems: Modeling and application.

Energy and Buildings, 40, 742–755.

KenGen, 2013: Well completion test report for OW-906. Kenya Electricity Generating Company, Ltd. – KenGen, Kenya, internal report, 3 pp.

Kjærnested, S.N., 2011: *A comparative study of geothermal pipeline route selection methods with visual effects optimization*. University of Iceland, Reykjavik, 57 pp.

Kristinsson, H., 2005: *Pipe route design using Variable Topography Distance Transforms.* University of Iceland, Reykjavík.

Lazalde-Crabtree, H., 1984: Design approach of steam-water separators and steam dryers for geothermal applications. *Geothermal Resource Council Bulletin, September* 1984, 11-20.

Mannvit, 2012: *Proposed field development plan for Greater Olkaria geothermal field*. Mannvit Consortium – consultancy services for geothermal resource optimisation study of Greater Olkaria geothermal fields, report 8, Kenya Electricity Generating Company Ltd. – KenGen, internal report, 59 pp.

Ofwona, C.O., 2010: Olkaria I reservoir response to 28 years of production. *Proceedings of the World Geothermal Congress 2010, Bali, Indonesia,* CD, 4 pp.

Onyango, S.O., 2015: Design of steam gathering system for Menengai geothermal field, Kenya. University of Iceland, Reykjavík, MSc thesis, UNU-GTP, report 1, 70 pp.

Ouma, P.A, 1992: *Steam gathering system for NE-Olkaria geothermal field, Kenya – preliminary design.* UNU-GTP, Iceland, report 9, 46 pp.

Ouma, P., 2010: Geothermal exploration and development of the Olkaria geothermal field. *Paper presented at Short Course V on Exploration for Geothermal Resources, organized by UNU-GTP, KenGen and GDC, Lake Bogoria and Naivasha, Kenya*, UNU-GTP SC-11, CD, 16 pp.

Purnanto, M.H., Zarrouk, S.J. and Cater, J.E., 2012: CFD modelling of two-phase flows inside geothermal steam-water separators. *Proceedings of the 34th New Zealand Geothermal Workshop, University of Auckland, Auckland, NZ,* 9 pp.

Tioga, 2014: *Pipe thicknesses.* Tioga Pipe – Pipe Supply Company, PH, USA, website: *www.tiogapipe.com.*

Umanzor, C., Hall, A., Buchanan, R., and Rosaria, N., 2015: Piping design considerations for geothermal steamfields. *Proceedings of the World Geothermal Congress 2015, Melbourne, Australia,* 9 pp.

Zarrouk, S.J. and Purnanto, M.H., 2014: Geothermal steam-water separators, *Geothermics, 53,* 236-254.

APPENDIX I: Pressure drop and diameter optimisation

Option 1 – Two-phase pipeline

Option 1 - Two-phase pipeline - DN800			
Wellhead pressure, P1	1.3	MPa	13bar
Separator pressure, P2	1.2	MPa	12bar
Allowable two-phase pressure drop, dP	0.1	MPa	
Total mass flow rate, m(t)	44	kg/s	
Dryness fration, x	0.28		
Pipe internal diameter, D	0.8	m	
Pipe cross-sectional area, A	0.503	m2	
Pipe roughness	0.000045	m	
Pipe relative roughness	0.000056		
Steam density, rho(g)	6.13	kg/m3	
Water density, rho(w)	878.35	kg/m3	
Steam discosity, mu(g)	0.0000153	kg/ms	
Water discosity, mu(w)	0.0001434	kg/ms	
Steam dass flow rate, m(s)	12.3	kg/s	
Water dass flow rate, m(w)	31.7	kg/s	
mu(w)/mu(g)	9.37	Less than 1000, Use Friedel	
Steam superficial velocity, v(s)	4.00	m/s	
Water superficial velocity, v(w)	0.07	m/s	
1. Friedel Method			
Two phase density, rho(tp)	21.51	kg/m3	
Surface tension, sigma	0.04	N/m	
Reynolds number steam, Re(s)	1281395		
Reynolds number water, Re(w)	351560		
Friction nactor steam, f(s)	0.0121		
Friction factor water, f(w)	0.0144		
Weber number, We	7018		
Froude number, Fr	2		
E	9.92		
F	0.34		
H	55.36		
Two phase multiplier (l)	90.89		
Two phase pressure drop	28.55	Pa/m	
Two phase pipe length	2970	m	
Additional length to cater for bends (15%)	445.5	m	
Total two phase pipe length	3415.5	m	
Total pressure drop (Pa)	97511.84	Pa	
Total pressure drop (mPA)	0.10	Mpa	

Option 2 – Two-phase pipeline

Option 2 - Two-phase pipeline - DN500			
Wellhead pressure, P1	1.3	MPa	13bar
Separator pressure, P2	1.2	MPa	12bar
Allowable two-phase pressure drop, dP	0.1	MPa	
Total mass flow rate, m(t)	44	kg/s	
Dryness fration, x	0.28		
Pipe internal diameter, D	0.5	m	
Pipe cross-sectional area, A	0.196	m2	
Pipe roughness	0.000045	m	
Pipe relative roughness	0.000090		
Steam density, rho(g)	6.13	kg/m3	
Water density, rho(w)	878.35	kg/m3	
Steam discosity, mu(g)	0.0000153	kg/ms	
Water discosity, mu(w)	0.0001434	kg/ms	
Steam dass flow rate, m(s)	12.3	kg/s	
Water dass flow rate, m(w)	31.7	kg/s	
mu(w)/mu(g)	9.37	Less than 1000, Use Friedel	
Steam superficial velocity, v(s)	10.23	m/s	
Water superficial velocity, v(w)	0.18	m/s	
1. Friedel Method			
Two phase density, rho(tp)	21.51	kg/m3	
Surface tension, sigma	0.04	N/m	
Reynolds number steam, Re(s)	2050232		
Reynolds number water, Re(w)	562497		
Friction nactor steam, f(s)	0.0111		
Friction factor water, f(w)	0.0132		
Weber number, We	28747		
Froude number, Fr	22		
E	9.98		
F	0.34		
H	55.36		
Two phase multiplier (l)	86.50		
Two phase pressure drop	261.01	Pa/m	
Two phase pipe length	2970	m	
Additional length to cater for bends (15%)	445.5	m	
Total two phase pipe length	3415.5	m	
Total pressure drop (Pa)	891487.72	Pa	
Total pressure drop (mPA)	0.89	Mpa	

Option 2 – Steam pipeline

Option 2 - Steam pipeline			
Wellhead pressure, P1	1.3	MPa	
Separator pressure, P2	1.2	MPa	
Allowable two-phase pressure drop, dP	0.1	MPa	
Total mass flow rate, m(t)	44	kg/s	
Dryness fration, x	0.28		
Pipe internal diameter, D	0.307	m	
Pipe cross-sectional area, A	0.074	m2	
Pipe roughness	0.000045	m	
Pipe relative roughness	0.000147		
Steam density, rho(g)	6.13	kg/m3	
Water density, rho(w)	878.35	kg/m3	
Steam discosity, mu(g)	0.0000153	kg/ms	
Water discosity, mu(w)	0.0001434	kg/ms	
Steam dass flow rate, m(s)	12.3	kg/s	
Water dass flow rate, m(w)	31.7	kg/s	
mu(w)/mu(g)	9.37	Less than 1000, Use Friedel	
Steam Velocity, v(s)	30	m/s	
Reynolds Number, Re	3690020		
Friction Factor	0.010		
Pressure Drop	8.58	Pa/m	
Steam pipe length	187	m	
Additional length to cater for bends (15%)	28.05	m	
Total Steam pipe length	215.05	m	
Total pressure drop	1845.474	Pa	
Total pressure drop	0.002	MPa	

APPENDIX II: Pipe wall thickness calculations

Option 1 - Pipe Thickness Work Sheet				
1. Two-phase - DN800				
Design pressure	2	mPa		
Pipe outer diameter, D	0.813	m		
Allowable stress, S	122.00	mPa		
Welding factor, E	1			
Temperature cofficient, y	0.4			
Corrosion allowance. A	0.003			
Minimum thickness, t	0.009620521	m		
Minimum thickness, t (mm)	9.62	mm		
Selected Thickness (mm)	12.7	mm		
Pipe OD (mm)	813.0		0.813	m
Pipe ID (mm)	787.6		0.788	m
Option 1 Summary				
Two phase pipe length	2970.00	m		
15% Addition for Bends	445.50	m		
Total Length	3415.50	m		
Two-phase pipe steel volume	94.85	m3		
Steel Density	7850.00	kg/m3		
Steel Mass	**744,541.35**	**kg**		
Steel cost/kg for DN800	**3.30**	**USD**		
Total Steel Cost	**2,456,986.47**	**USD**		
Option 2 - Pipe Thickness Work Sheet				
1. Two-phase - DN500				
Design Pressure	2	mPa		
Pipe Outer Diameter, D	0.508	m		
Allowable Stress, S	122.00	mPa		
Welding Factor, E	1			
Temperature cofficient, y	0.4			
Corrosion Allowance, A	0.003	m		
Minimum thickness, t	0.007136808	m		
Minimum thickness, t (mm)	7.14	mm		
Selected thickness (mm)	9.53	mm		
Pipe OD (mm)	508.00		0.508	m
Pipe ID (mm)	488.94		0.489	m
2. Steam - DN300				
Design pressure	2	mPa		
Pipe outer diameter, D	0.32	m		
Allowable stress, S	122.00	mPa		
Welding factor, E	1			
Temperature cofficient, y	0.4			
Corrosion allowance. A	0.003	m		
Minimum thickness, t	0.005630293	m		
Minimum thickness, t	5.63	mm		
Selected thickness (mm)	6.35	mm		
Pipe OD (mm)	323.85		0.32385	m
Pipe ID (mm)	311.15		0.31115	m
Option 2 Summary				
Two phase pipe length	100.00	m		
15% Addition for Bends	15.00	m		
Total two phase pipe Length	115.00	m		
Two-phase pipe steel volume	1.72	m3		
Steel density	7850.00	kg/m3		
Mass two phase pipe	13474.28	kg		
Steam pipe length	187.00	m		
15% Addition for bends	28.05	m		
Total steam pipe length	215.05	m		
Steam pipe steel volume	1.36	m3		
Mass steam pipe	10693.82	kg		
Total Steel Mass	**24168.10**	**kg**		
Total Steel Cost	**60,574.27**	**USD**		

APPENDIX III: Separator dimensions and wall thicknesses

Separator Design Work Sheet				
Separation pressure	1.2	mPa		
Steam density@12bar	6.13	kg/m3		
Water density@12bar	878.4	kg/m3		
Design pressure CL150	2.0	mPa		
Mass flow rate steam, m	12	kg/s		
Volumetric flow rate, Qvs	1.96	m3/s		
Steam velocity (outlet)	30	m/s		
Flow area, A	0.065252855	m3		
Diameter, Dt	0.288221692	m		
	Bangma	**Lazalde -Crabtree**	**Spiral Inlet**	**Unit**
D	0.86	0.95	**0.9**	m
D_e	0.23	0.29	**0.3**	m
D_b	0.29	0.29	**0.2**	m
α	0.94	0.04	**0.1**	m
β	0.86	1.01	**1.0**	m
Z	0.86	1.59	**1.7**	m
L_T	2.02	1.87	**2.0**	m
L_B	1.30	1.43	**1.5**	m
Separator Wall Thickness				
Allowable stress, S	122	mPa		
Welding factor, E	1			
Temperature cofficient, y	0.4			
Corrosion allowance, A	0.003			
	Bangma	**Lazalde -Crabtree**	**Spiral Inlet**	
Minimum thickness, tm	0.010	0.011	0.010	m
Overal height, H	3.31	3.30	3.51	m
Ellipse short radius, b	0.22	0.24	0.22	m
Ellipse long radius, a	0.43	0.48	0.44	m
Ellipse surface area	0.29	0.36	0.30	m2
Cylinder surface area	9.00	9.86	9.76	m2
Total surface area	9.30	10.22	10.06	m2
Volume of steel, V	0.12	0.13	0.13	m3
Density of steel	7850			kg/m3
Weight of steel (rhoX volume)	927.02	1018.65	1002.98	kg
Cost/kg	3.3		**3.3**	USD
Total Cost	**3059.16**	**3361.53**	**3309.83**	**USD**

APPENDIX IV: Pipe stress analysis calculations

Two-phase pipeline

1. Two Phase pipeline - DN500				
Nominal diameter	500	mm	0.5000	m
Outside diameter	508	mm	0.5080	m
Inside diameter	288	mm	0.2880	m
Pipe thickness	110	mm	0.1100	m
Insulation thickness	30	mm	0.0300	m
Insulation diameter (De)	568	mm	0.5680	m
Cladding thickness	2	mm	0.002	m
Cladding diameter (Dc)	572	mm	0.572	m
Steel density	7850	kg/m3		
Insulation density	400	kg/m3		
Cladding density	2700	kg/m3		
Pipe weight (Qp)	10593.0	N/m		
Insulation weight (Qe)	199.0	N/m		
Cladding weight (Qc)	95.8	N/m		
Vertical sustained load (Qp+Qe+Qc)	**10887.9**	**N/m**		
Media density	21.5	kg/m3		
Seismic factor	0.16			
Wind velocity (Vw)	30	m/s		
Wind form factor, C	0.6			
Wind pressure (p) = Vw^2/1.6	562.5			
Media weight (Qm)	13.7	N/m		
Vertical seismic load (Qsv)	872.1	N/m		
Vertical occasional load (Qm+Qsv)	**885.9**	**N/m**		
Horizontal seismic load (Qsh)	**1745.5**	N/m		
Wind load (Qw) = C*p*Dc	**193.1**	N/m		
Horizontal occasional load	**1745.5**	N/m		
Design pressure	11000000	mPa		
Max allowable stress, hot (sh)	122000000	mPa		
Load factor (k)	1			
	109300000	A		
	0.046907956	B		
	6525.414765	C		
Length between supports SQRT{(A*B)/C}	**28.03**	**m**		
Youngs modulus E	2E+11	Pa		
Uniform load (Qp+Qe+Qc)	10887.9	N/m		
Moment of inertia I	0.002931747	m4		
Allowable deflection, m	0.002204517	m		
Allowable deflection, mm	2	mm		

Steam pipeline

2. Steam pipeline				
Nominal diameter	300	mm	0.3000	m
Outside diameter	323	mm	0.3230	m
Inside diameter	311	mm	0.3110	m
Pipe thickness	6	mm	0.0060	m
Insulation thickness	30	mm	0.0300	m
Insulation diameter (De)	383	mm	0.3830	m
Cladding thickness	2	mm	0.002	m
Cladding diameter (Dc)	387	mm	0.387	m
Steel density	7850	kg/m3		
Insulation density	400	kg/m3		
Cladding density	2700	kg/m3		
Pipe weight (Qp)	460.2	N/m		
Insulation weight (Qe)	130.6	N/m		
Cladding weight (Qc)	64.7	N/m		
Vertical sustained load (Qp+Qe+Qc)	**655.5**	**N/m**		
Media density	6.13	kg/m3		
Seismic factor	0.16			
Wind velocity (Vw)	30	m/s		
Wind form factor ©	0.6			
Wind pressure (p) = Vw^2/1.6	562.5			
Media weight (Qm)	4.6	N/m		
Vertical seismic load (Qsv)	52.8	N/m		
Vertical occasional load (Qm+Qsv)	**57.4**	**N/m**		
Horizontal seismic load (Qsh)	**105.9**	N/m		
Wind load (Qw) = C*p*Dc	**130.6**	N/m		
Horizontal occasional load	**130.6**	**N/m**		
Design pressure	2000000	Pa		
Max allowable stress, hot (sh)	122000000	Pa		
Load factor (k)	1			
	95083333.33	A		
	0.001201492	B		
	257.8084604	C		
Length between supports SQRT{(A*B)/C}	**21.05**	**m**		
Youngs modulus E	2E+11	Pa		
Uniform load (Qp+Qe+Qc)	655.5	N/m		
Moment of inertia I	7.50932E-05	m4		
Allowable deflection, m	0.002194722	m		
Allowable deflection, mm	2	mm		

APPENDIX V: Pipe thicknesses and costs (Tioga, 2014)

Tioga™

Philadelphia Regional Center
2450 Wheatsheaf Lane
Philadelphia, PA 19137
O 215-831-0700
F 215-533-1645
E sales@tiogapipe.com

Houston Regional Center
616 FM 1960 W, Suite 700
Houston, TX 77090
O 713-433-2111
F 281-397-0132
E sales@tiogapipe.com

Chattanooga Regional Center
1301 Riverfront Parkway, Suite 108
Chattanooga, TN 37402
O 423-899-3398
F 423-899-9695
E sales@tiogapipe.com

PIPE DIMENSIONS AND WEIGHTS

Available in commercial and nuclear

U.S./METRIC

NOMINAL PIPE SIZE	OD	SCHEDULE DESIGNATIONS			WALL THICKNESS		WEIGHT		ID	
INCH MM	INCH MM	ASME			INCH	MM	LBS/ FOOT	KG/ METER	INCH	MM
1/8 6	0.405 10.3	10 STD XS	40 80	10S 40S 80S	0.049 0.068 0.095	1.24 1.73 2.41	0.19 0.24 0.31	0.28 0.37 0.47	0.307 0.269 0.215	7.82 6.84 5.84
1/4 8	0.540 13.7	10 STD XS	40 80	10S 40S 80S	0.065 0.088 0.119	1.65 2.24 3.02	0.33 0.43 0.54	0.49 0.63 0.80	0.410 0.364 0.302	10.40 9.22 7.66
3/8 10	0.675 17.1	10 STD XS	40 80	10S 40S 80S	0.065 0.091 0.126	1.65 2.31 3.20	0.42 0.57 0.74	0.63 0.84 1.10	0.545 0.493 0.423	13.80 12.48 10.70
1/2 15	0.840 21.3	5 10 STD XS 160 XX	40 80	5S 10S 40S 80S	0.065 0.083 0.109 0.147 0.188 0.294	1.65 2.11 2.77 3.73 4.78 7.47	0.54 0.67 0.85 1.09 1.31 1.72	0.80 1.00 1.27 1.62 1.95 2.55	0.710 0.674 0.622 0.546 0.464 0.252	18.00 17.08 15.76 13.84 11.74 6.36
3/4 20	1.050 26.7	5 10 STD XS 160 XX	40 80	5S 10S 40S 80S	0.065 0.083 0.113 0.154 0.219 0.308	1.65 2.11 2.87 3.91 5.56 7.82	0.69 0.86 1.13 1.48 1.95 2.44	1.03 1.28 1.69 2.20 2.90 3.64	0.920 0.884 0.824 0.742 0.612 0.434	23.40 22.48 20.96 18.88 15.58 11.06
1 25	1.315 33.4	5 10 STD XS 160 XX	40 80	5S 10S 40S 80S	0.065 0.109 0.133 0.179 0.250 0.358	1.65 2.77 3.38 4.55 6.35 9.09	0.87 1.41 1.68 2.17 2.85 3.66	1.29 2.09 2.50 3.24 4.24 5.45	1.185 1.097 1.049 0.957 0.815 0.599	30.10 27.86 26.64 24.30 20.70 15.22
1-1/4 32	1.660 42.2	5 10 STD XS 160 XX	40 80	5S 10S 40S 80S	0.065 0.109 0.140 0.191 0.250 0.382	1.65 2.77 3.56 4.85 6.35 9.70	1.11 1.81 2.27 3.00 3.77 5.22	1.65 2.69 3.39 4.47 5.61 7.77	1.530 1.442 1.380 1.278 1.160 0.896	38.90 36.66 35.08 32.50 29.50 22.80
1-1/2 40	1.900 48.3	5 10 STD XS 160 XX	40 80	5S 10S 40S 80S	0.065 0.109 0.145 0.200 0.281 0.400	1.65 2.77 3.68 5.08 7.14 10.15	1.28 2.09 2.72 3.63 4.86 6.41	1.90 3.11 4.05 5.41 7.25 9.55	1.770 1.682 1.610 1.500 1.338 1.100	45.00 42.76 40.94 38.14 34.02 28.00
2 50	2.375 60.3	5 10 STD XS 160 XX	40 80	5S 10S 40S 80S	0.065 0.109 0.154 0.218 0.344 0.436	1.65 2.77 3.91 5.54 8.74 11.07	1.61 2.64 3.66 5.03 7.47 9.04	2.39 3.93 5.44 7.48 11.11 13.44	2.245 2.157 2.067 1.939 1.687 1.503	57.00 54.76 52.48 49.22 42.82 38.16
2-1/2 65	2.875 73.0	5 10 STD XS 160 XX	40 80	5S 10S 40S 80S	0.083 0.120 0.203 0.276 0.375 0.552	2.11 3.05 5.16 7.01 9.53 14.02	2.48 3.53 5.80 7.67 10.02 13.71	3.69 5.26 8.63 11.41 14.92 20.39	2.709 2.635 2.469 2.323 2.125 1.771	68.78 66.90 62.68 58.98 53.94 44.96
3 80	3.500 88.9	5 10 STD XS 160 XX	40 80	5S 10S 40S 80S	0.083 0.120 0.216 0.300 0.438 0.600	2.11 3.05 5.49 7.62 11.13 15.24	3.03 4.34 7.58 10.26 14.34 18.60	4.52 6.46 11.29 15.27 21.35 27.68	3.334 3.260 3.068 2.900 2.624 2.300	84.68 82.80 77.92 73.66 66.64 58.42
3-1/2 90	4.000 101.6	5 10 STD XS XX	40 80	5S 10S 40S 80S	0.083 0.120 0.226 0.318 0.636	2.11 3.05 5.74 8.08 16.15	3.48 4.98 9.12 12.52 22.87	5.18 7.41 13.57 18.64 34.03	3.834 3.760 3.548 3.364 2.728	97.38 95.50 90.12 85.44 69.30
4 100	4.500 114.3	5 10 STD XS 120 160 XX	40 80	5S 10S 40S 80S	0.083 0.120 0.156 0.188 0.237 0.337 0.438 0.531 0.674	2.11 3.05 3.96 4.78 6.02 8.56 11.13 13.49 17.12	3.92 5.62 7.24 8.67 10.80 15.00 19.02 22.53 27.57	5.84 8.37 10.78 12.91 16.08 22.32 28.32 33.54 41.03	4.334 4.260 4.188 4.124 4.026 3.826 3.624 3.438 3.152	110.08 108.20 106.38 104.74 102.26 97.18 92.04 87.32 80.06
4-1/2 115	5.000 127.0	STD XS XX	40 80	40S 80S	0.247 0.355 0.710	6.27 9.02 18.03	12.55 17.63 32.56	18.67 26.24 48.45	4.506 4.290 3.580	114.46 108.96 90.94

NOMINAL PIPE SIZE	OD	SCHEDULE DESIGNATIONS			WALL THICKNESS		WEIGHT		ID	
INCH MM	INCH MM	ASME			INCH	MM	LBS/ FOOT	KG/ METER	INCH	MM
5 125	5.563 141.3	5 10 STD XS 120 160 XX	40 80	5S 10S 40S 80S	0.109 0.134 0.258 0.375 0.500 0.625 0.750	2.77 3.40 6.55 9.53 12.70 15.88 19.05	6.36 7.78 14.63 20.80 27.06 32.99 38.59	9.46 11.56 21.77 30.97 40.28 49.12 57.43	5.345 5.295 5.047 4.813 4.563 4.313 4.063	135.76 134.50 128.20 122.24 115.90 109.54 103.20
6 150	6.625 168.3	5 10 STD XS 120 160 XX	40 80	5S 10S 40S 80S	0.109 0.134 0.188 0.280 0.432 0.562 0.719 0.864	2.77 3.40 4.78 7.11 10.97 14.27 18.26 21.95	7.59 9.30 12.94 18.99 28.60 36.43 45.39 53.21	11.31 13.83 19.28 28.26 42.56 54.21 67.57 79.22	6.407 6.357 6.249 6.065 5.761 5.501 5.187 4.897	162.76 161.50 158.74 154.08 146.36 139.76 131.78 124.40
7 175	7.625 193.7	STD XS XX	40 80	40S 80S	0.301 0.500 0.875	7.65 12.70 22.23	23.57 38.08 63.14	35.10 56.69 94.00	7.023 6.625 5.875	178.40 168.30 149.24
8 200	8.625 219.1	 10 20 30 STD 60 XS 100 120 140 XX 160	 40 80 	5S 10S 40S 80S 	0.109 0.148 0.250 0.277 0.322 0.406 0.500 0.594 0.719 0.812 0.875 0.906	2.77 3.76 6.35 7.04 8.18 10.31 12.70 15.09 18.26 20.62 22.23 23.01	9.92 13.41 22.38 24.72 28.58 35.67 43.43 51.00 60.77 67.82 72.49 74.76	14.78 19.97 33.32 36.82 42.55 53.09 64.64 75.92 90.44 100.93 107.93 111.27	8.407 8.329 8.125 8.071 7.981 7.813 7.625 7.437 7.187 7.001 6.875 6.813	213.56 211.58 206.40 205.02 202.74 198.48 193.70 188.92 182.58 177.86 174.64 173.08
9 225	9.625 244.5	STD XS XX	40 80	40S 80S	0.342 0.500 0.875	8.69 12.70 22.23	33.94 48.77 81.85	50.54 72.60 121.85	8.941 8.625 7.875	227.12 219.10 200.04
10 250	10.750 273.0	 20 30 STD XS 80 100 120 140 160	 40 60 XX 	5S 10S 40S 80S 	0.134 0.165 0.188 0.250 0.307 0.365 0.500 0.594 0.719 0.844 1.000 1.125	3.40 4.19 4.78 6.35 7.80 9.27 12.70 15.09 18.26 21.44 25.40 28.58	15.21 18.67 21.23 28.06 34.27 40.52 54.79 64.49 77.10 89.38 104.23 115.75	22.61 27.78 31.62 41.76 51.01 60.29 81.53 95.98 114.71 133.01 155.10 172.27	10.482 10.420 10.374 10.250 10.136 10.020 9.750 9.562 9.312 9.062 8.750 8.500	266.20 264.62 263.44 260.30 257.40 254.46 247.60 242.82 236.48 230.12 222.20 215.84
11 275	11.750 298.5	STD XS XX	40 80	40S 80S	0.375 0.500 0.875	9.53 12.70 22.23	45.60 60.13 101.72	67.91 89.51 151.46	11.000 10.750 10.000	279.44 273.10 254.04
12 300	12.750 323.8	 20 30 STD XS 60 80 100 120 140 160	 XX 	5S 10S 40S 80S 	0.156 0.180 0.188 0.250 0.330 0.375 0.406 0.500 0.562 0.688 0.844 1.000 1.125 1.312	3.96 4.57 4.78 6.35 8.38 9.53 10.31 12.70 14.27 17.48 21.44 25.40 28.58 33.32	21.00 24.19 25.25 33.41 43.81 49.61 53.57 65.48 73.22 88.71 107.42 125.61 139.81 160.42	31.24 35.98 37.61 49.71 65.19 73.86 79.71 97.44 108.93 132.05 159.87 186.92 208.08 238.69	12.438 12.390 12.374 12.250 12.090 12.000 11.938 11.750 11.626 11.374 11.062 10.750 10.500 10.126	315.88 314.66 314.24 311.10 307.04 304.74 303.18 298.40 295.26 288.84 280.92 273.00 266.64 257.16
14 350	14.000 355.6	 10 20 STD 40 XS 60 80 100 120 140 160	 30 	10S 40S 80S 	0.188 0.250 0.312 0.375 0.438 0.500 0.594 0.750 0.938 1.094 1.250 1.406	4.78 6.35 7.92 9.53 11.13 12.70 15.09 19.05 23.83 27.79 31.75 35.71	27.76 36.75 45.65 54.62 63.50 72.16 85.13 106.23 130.98 150.93 170.37 189.29	41.36 54.69 67.91 81.33 94.55 107.40 126.72 158.11 194.98 224.66 253.58 281.72	13.624 13.500 13.376 13.250 13.124 13.000 12.812 12.500 12.124 11.812 11.500 11.188	346.04 342.90 339.76 336.54 333.34 330.20 325.42 317.50 307.94 300.02 292.10 284.18

NOMINAL PIPE SIZE	OD	SCHEDULE DESIGNATIONS	WALL THICKNESS		WEIGHT		ID	
INCH MM	INCH MM	ASME	INCH	MM	LBS/ FOOT	KG/ METER	INCH	MM
16 400	16.000 406.4	10S	0.188	4.78	31.78	47.34	15.624	396.84
		10	0.250	6.35	42.09	62.65	15.500	393.70
		20	0.312	7.92	52.32	77.83	15.376	390.56
		STD 30 40S	0.375	9.53	62.64	93.27	15.250	387.34
		XS 40 80S	0.500	12.70	82.85	123.31	15.000	381.00
		60	0.656	16.66	107.60	160.13	14.688	373.08
		80	0.844	21.44	136.74	203.54	14.312	363.52
		100	1.031	26.19	164.98	245.57	13.938	354.02
		120	1.219	30.96	192.61	286.66	13.562	344.48
		140	1.438	36.53	223.85	333.21	13.124	333.34
		160	1.594	40.49	245.48	365.38	12.812	325.42
18 450	18.000 457	10S	0.188	4.78	35.80	53.31	17.624	447.44
		10	0.250	6.35	47.44	70.57	17.500	444.30
		20	0.312	7.92	58.99	87.71	17.376	441.16
		STD 40S	0.375	9.53	70.65	105.17	17.250	437.94
		30	0.438	11.13	82.23	122.38	17.124	434.74
		XS 80S	0.500	12.70	93.54	139.16	17.000	431.60
		40	0.562	14.27	104.76	155.81	16.876	428.46
		60	0.750	19.05	138.30	205.75	16.500	418.90
		80	0.938	23.83	171.08	254.57	16.124	409.34
		100	1.156	29.36	208.15	309.64	15.688	398.28
		120	1.375	34.93	244.37	363.58	15.250	387.14
		140	1.562	39.67	274.48	408.28	14.876	377.66
		160	1.781	45.24	308.79	459.39	14.438	366.52
20 500	20.000 508	10S	0.218	5.54	46.10	68.61	19.564	496.92
		10	0.250	6.35	52.78	78.56	19.500	495.30
		STD 20 40S	0.375	9.53	78.67	117.15	19.250	488.94
		XS 30 80S	0.500	12.70	104.23	155.13	19.000	482.60
		40	0.594	15.09	123.23	183.43	18.812	477.82
		60	0.812	20.62	166.56	247.84	18.376	466.76
		80	1.031	26.19	209.06	311.19	17.938	455.62
		100	1.281	32.54	256.34	381.55	17.438	442.92
		120	1.500	38.10	296.65	441.52	17.000	431.80
		140	1.750	44.45	341.41	508.15	16.500	419.10
		160	1.969	50.01	379.53	564.85	16.062	407.98
22 550	22.000 559	10S	0.218	5.54	50.76	75.55	21.564	547.92
		10	0.250	6.35	58.13	86.55	21.500	546.30
		STD 20 40S	0.375	9.53	86.69	129.14	21.250	539.94
		XS 30 80S	0.500	12.70	114.92	171.10	21.000	533.60
		60	0.875	22.23	197.60	294.27	20.250	514.54
		80	1.125	28.58	251.05	373.85	19.750	501.84
		100	1.375	34.93	303.16	451.45	19.250	489.14
		120	1.625	41.28	353.94	527.05	18.750	476.44
		140	1.875	47.63	403.38	600.67	18.250	463.74
		160	2.125	53.98	451.49	672.30	17.750	451.04

NOMINAL PIPE SIZE	OD	SCHEDULE DESIGNATIONS	WALL THICKNESS		WEIGHT		ID	
INCH MM	INCH MM	ASME	INCH	MM	LBS/ FOOT	KG/ METER	INCH	MM
24 600	24.000 610	10 10S	0.250	6.35	63.47	94.53	23.500	597.30
		STD 20 40S	0.375	9.53	94.71	141.12	23.250	590.94
		XS 80S	0.500	12.70	125.61	187.07	23.000	584.60
		30	0.562	14.27	140.81	209.65	22.876	581.46
		40	0.688	17.48	171.45	255.43	22.624	575.04
		60	0.969	24.61	238.57	355.28	22.062	560.78
		80	1.219	30.96	296.86	442.11	21.562	548.08
		100	1.531	38.89	367.74	547.74	20.938	532.22
		120	1.812	46.02	429.79	640.07	20.376	517.96
		140	2.062	52.37	483.57	720.19	19.876	505.26
		160	2.344	59.54	542.64	808.27	19.312	490.92
26 650	26.000 660	10	0.312	7.92	85.68	127.36	25.376	644.16
		STD 40S	0.375	9.53	102.72	152.88	25.250	640.94
		XS 80S	0.500	12.70	136.30	202.74	25.000	634.60
28 700	28.000 711	10	0.312	7.92	92.35	137.32	27.376	695.16
		STD 40S	0.375	9.53	110.74	164.86	27.250	691.94
		XS 20 80S	0.500	12.70	146.99	218.71	27.000	685.60
		30	0.625	15.88	182.90	272.23	26.750	679.24
30 750	30.000 762	10	0.312	7.92	99.02	147.29	29.376	746.16
		STD 40S	0.375	9.53	118.76	176.85	29.250	742.94
		XS 20 80S	0.500	12.70	157.68	234.68	29.000	736.60
		30	0.625	15.88	196.26	292.20	28.750	730.24
32 800	32.000 813	10	0.312	7.92	105.69	157.25	31.376	797.16
		STD	0.375	9.53	126.78	188.83	31.250	793.94
		XS 20	0.500	12.70	168.37	250.65	31.000	787.60
		30	0.625	15.88	209.62	312.17	30.750	781.24
		40	0.688	17.48	230.29	342.94	30.624	778.04
34 850	34.000 864	10	0.312	7.92	112.36	167.21	33.376	848.16
		STD	0.375	9.53	134.79	200.82	33.250	844.94
		XS 20	0.500	12.70	179.06	266.63	33.000	838.60
		30	0.625	15.88	222.99	332.14	32.750	832.24
		40	0.688	17.48	245.00	364.92	32.624	829.04
36 900	36.000 914	10	0.312	7.92	119.03	176.97	35.376	898.16
		STD	0.375	9.53	142.81	212.57	35.250	894.94
		XS	0.500	12.70	189.75	282.29	35.000	888.60
42 1050	42.000 1067	STD	0.375	9.53	166.86	248.53	41.250	1047.94
		XS	0.500	12.70	221.82	330.21	41.000	1041.60
			0.625	15.88	276.44	411.64	40.750	1035.24
			0.750	19.05	330.72	492.33	40.500	1028.90
48 1200	48.000 1219	STD	0.375	9.53	190.92	284.25	47.250	1199.94
		XS	0.500	12.70	253.89	377.81	47.000	1193.60

PIPING • TUBING • FITTINGS FLANGES • RELATED PRODUCTS

Type	Seamless & Welded
Commodity	Chrome • Stainless • Carbon • Low Temperature
Specifications	A/SA335 • A/SA312 • A/SA213 • A/SA106 • A/SA53/API5L • A/SA333
Sizes (O.D.)	1/8" (3.175mm) - 60" (1524mm) (Larger ODs Available)
Grades	Chrome: P1 • P5 • P9 • P11 • P22 • P91 Stainless: 304 • 304H • 304L • 316 • 316H • 316L • 316LN • 321 • 321H • 347 • 347H • 310 • 310s • 309 • Alloy 20 Low Temp: Grade 1/6 • Grade 3 Carbon: Grade B • Grade C • Galvanized

MILITARY SPEC PIPE & TUBING

Program	MIL-I-45208A Quality Program • Approved Level 1 Supplier
Contact Tioga for	U.S. Navy Specifications • Navy Nuclear • MIC Level 1 • Ultrasonic Testing
Fittings & Flanges	All Fittings & Flanges to Match the Pipe

NUCLEAR MATERIALS

Program	ASME Section III - ASME QSC 467
Specifications	10CFR50 Appendix B • N45.2 • NQA-1 • U.S. Navy Nuclear Specifications
Products	Pipe • Tubing • Fittings • Flanges • Structurals • Fasteners • Forgings • Castings • Weld Rod • Plate
Grades	Carbon • Stainless • Chrome Moly • Nickel Alloys • Duplex • 6 Moly Alloys • Low Temperature • Special Melts • Copper & Titanium

SPECIALTY ALLOYS

Type	Seamless & Welded
Commodity	Nickel • Duplex & Titanium
Specifications & Grades	Alloy 800 • Alloy 825 • Alloy 600 • Alloy 625 • Alloy 400 • 6% Moly Grades • Duplex A790 UNS 31803 • 316LN
Sizes (O.D.)	1/8" (3.175mm) - 8" (203.2mm)
Wall Dimensions	0.035" (.889mm) - 0.875" (22.23mm)

TIOGA SPECIALTIES

- Project Management
- 24/7 Emergency Service
- Just-In-Time Programs
- Inventory in Stock
- All Schedule Walls
- Special Heavy Walls to 4" (101.6mm)
- Header Pipe to 4" Wall (101.6mm)
- Special Intermediate Walls
- Average & Minimum Walls
- Saw Cut up to 40" (1016mm)
- Cutting: Square & Miter
- Custom Lengths and OD's
- End Preps-Various
- Hard to Find Metals & Sizes
- Se Habla Español
- Exceptional Mill/Sourcing Relations
- Dedicated Project Solution Teams
- Vendor Managed Inventory Programs
- Mobile On-Site Inventory Programs
- Quick Response Programs
- Low Total Cost Solutions
- International Export & Packaging
- EN PED 97/23/EC
- ISO 9001-2008
- MIC Level 1 Supplier
- In-House Testing
- Destructive Examination
- Non-Destructive Examination
- In-House Hydrostatic Testing
- Full EDI Capabilities
- Customized e-business Solutions
- Emergency Forged and Buttweld Fittings

Note: Actual dimensions can vary from the figures based on specifications/manufacturing tolerances. The Data for weight is based on the following calculation for wrought steel pipe:
LB/Foot = (Outside diameter [in.] – Wall Thickness [in.]) x (Wall Thickness [in.]) x (10.69)
KG/Meter = (Outside diameter [mm] – Wall Thickness [mm]) x (Wall Thickness [mm]) x (0.0246615)